UNPUBLISHED PRELIMINARY DATA

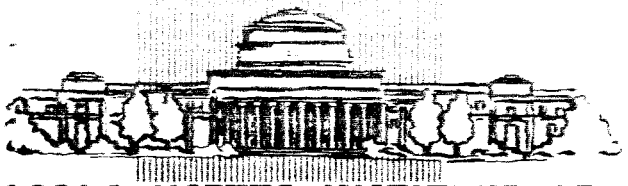

MASSACHUSETTS INSTITUTE OF TECHNOLOGY

N64-26596
Code-1 Cat. 10
Grant NsG-581-62

T-64-1

THE DESIGN AND CONSTRUCTION OF AN ACCELERATION CART

by

Richard T. Schulze, 1st Lt., USAF
Russell E. Freeland, Jr., Capt., USAF

June 1964

Master of Science Thesis

MAN-VEHICLE CONTROL LABORATORY
CENTER FOR SPACE RESEARCH
MASSACHUSETTS INSTITUTE OF TECHNOLOGY
CAMBRIDGE, MASSACHUSETTS 02139

REPORTS CONTROL

THE DESIGN AND CONSTRUCTION OF AN ACCELERATION CART

by

RICHARD J. SCHULTE 1/Lt. USAF
S.B., South Dakota State University
(1962)

RUSSELL ELIAS VREELAND JR. CAPTAIN USAF
S.B., United States Naval Academy
(1958)

SUBMITTED IN PARTIAL FULFILLMENT
OF THE REQUIREMENTS FOR THE
DEGREE OF MASTER OF SCIENCE

at the

MASSACHUSETTS INSTITUTE OF TECHNOLOGY
June, 1964

Signature of Author/s Richard J. Schulte

Russell E. Vreeland Jr.

Department of Aeronautics and Astronautics, June 1964

Certified by Laurence R. Young
Thesis Supervisor

Accepted by Judson R. Baron
Chairman, Departmental
Graduate Committee

THE DESIGN AND CONSTRUCTION OF AN ACCELERATION CART

by

Richard J. Schulte

Russell Elias Vreeland Jr.

Submitted to the Department of Aeronautics and Astronautics on 22 May 1964 in partial fulfillment of the requirements for the degree of Master of Science.

26596

ABSTRACT

This thesis presents a discussion of the problems encountered in designing and constructing a simulator to determine human vestibular response to a range of linear accelerations from 0-.3g's. Starting with a set of initial performance specifications, the designers have combined an array of commercially available components into a system, which, although requiring further refinements before completion, shows considerable promise of fulfilling the initial requirements.

The resulting system consists of a wheeled vehicle, driven by a cable and drum arrangement, powered by a hydraulic pump and motor, and controlled by a hydraulic-electric servo valve. Technical design considerations are presented along with a discussion of the "trade-offs" between various component options. A description of the system characteristics as well as an analysis of preliminary test results and recommendations for future system improvements are included.

author

Thesis Supervisor: Laurence R. Young

Title: Assistant Professor of Aeronautics and Astronautics

ACKNOWLEDGEMENTS

This thesis was undertaken as part of the National Aeronautics and Space Administration project No. NSG-577. The authors wish to express their appreciation to the following persons: Professor Laurence R. Young, and Mr. Jacob Meiry, for their invaluable assistance and encouragement, Mr. Oscar Wallin, without whose advice the construction of the vehicle would not have been possible, and Mrs. Mary Vreeland and Mrs. Barbara Marks, who typed the manuscript.

TABLE OF CONTENTS

Chapter No.		Page No.
1	Introduction	1
2	Design of the Power and Control System	5
3	Vehicle Design	11
4	Test Results and Conclusions	28
Appendices		
A	Calculation of power required to accelerate a 400 pound mass	37
B	Comparison of methods for control power transmission	45
C	Derivation of the speed and torque requirements at the load drum shaft	49
D	The drive system design	52
E	Determination of the hydraulic component parameters	57
F	Vibration calculations	63
G	Structural calculations	68
H	Safety device calculations	71
I	Test data	74
Figures		
1	Pump assembly	79
2	Motor and drive assembly	80
3	Dummy pulley	81
4	Assembled vehicle	82
5	Vehicle carriage	83
6	Guide vanes	84
7	Wheel mount	85
References		86

CHAPTER 1

INTRODUCTION

This thesis is concerned with a small segment of a larger project, the overall purpose of which is to arrive at a quantitative engineering description of the human operator in his role as a component in closed loop control systems. With a description of human responses to visual, tactile and vestibular inputs control system compensation may be designed to optimize effectively the overall system performance.

The segment of the project dealt with in this thesis concerns the design and construction of a device to be used in determining the human response to inputs of linear acceleration along a single axis of motion. This required the isolation of the test subject from all other disturbances, restricting his sensory perception capability to vestibular inputs. The word "vestibular" refers to the ability of sensors, located in the inner ear, to detect and measure the direction and magnitude of applied linear and angular accelerations.(1) It is the accuracy of this measurement capability, and the human response to it, which remains to be quantitatively determined.

The following specifications for the device were established by the user as those to be met by a final successful design:

(a) The normal weight of the vehicle, with the subject and associated test equipment aboard, was established at 300 pounds. This can be roughly

broken down into:

(1) Vehicle weight 100 pounds

(2) Subject weight 200 pounds

This number represented an estimate of the minimum weight to be accelerated by the power system and also served as a maximum total weight goal for the vehicle design.

(b) A peak acceleration amplitude was established as .3g's (9.66 ft/sec^2).

It should be noted here that this reflects the project's purpose of studying vestibular responses to relatively low amplitude accelerations, such as would be encountered in a vehicle orientation maneuver, rather than any desire to study human "g" tolerance. The accelerations were to be directed along a single horizontal axis, with the additional requirement that the subject could be oriented on the device at any angle to the line of motion from 0° to 360° and in any position from 90° sitting to full prone.

(c) The minimum acceleration level to be provided by the device was established at .01g which represented the best estimates of the minimum human perception level or threshold.

(d) The threshold level of human perception of acceleration also established the maximum level of the cross axis disturbance which could be tolerated. In effect, this amounted to a vibration isolation problem, restricting transverse and vertical vibratory accelerations to a level below .01g. In addition, it was required that angular accelerations be limited to less than 2 degrees per second squared, the threshold level for human perception of angular accelerations.

(e) Although the device was required to respond to random inputs, a sinusoidal response capability over a range from zero to one cycle per second was established as an adequate design criteria.

(f) The final specification to be established was the maximum amplitude of the response. This was limited, by the amount of physical space available for the equipment, to a 32 ft peak-to-peak displacement, leaving a four foot overrun at each end of the track, the total space available being constrained to approximately 40 ft.

The specifications outlined above served as the initial conditions for the designers' attack on the problem. The requirement to isolate the test subject from angular accelerations of greater than 2 degrees/sec^2 caused the early rejection of proposals for a swing or centrifuge configuration, and focused attention on the use of sliding or wheeled vehicles. Almost immediately considerations were further narrowed to wheeled vehicles, since the power required to overcome the frictional resistance encountered in sliding devices would be excessive.

The complete design problem presented many areas for investigation. The areas of principal concern were those of power, control, and vibration isolation. Many subsidiary investigations had to be made into such design considerations as structural loading and natural frequency; power transmission to the vehicle, including the design of shafting and shaft couplings, selection of the transmission mechanism (cable, belt, chain, worm gears etc.), and calculation of bearing loads; a simple but effective guidance system; and safety. Perhaps the greatest problems encountered in the design phase were the problems of locating "off the shelf" commercially available components which could be combined into a feasible system, and finding the

necessary technical data, required for design purposes, on commercial items which were available.

This chapter is followed by three major sections. Chapter two with its associated appendices, discusses the design of the power and control systems, and presents the factors which were considered in this process, the "trade-offs" which were made, and the governing reasons behind the selection of each system component. Chapter three presents a similar discussion of the vehicle design process. The fourth and final chapter includes an analysis of some preliminary tests of the control system, and recommends modifications which could be made to both the vehicle and the power and control designs in order to improve overall system performance.

CHAPTER 2

DESIGN OF THE POWER AND CONTROL SYSTEM

The task presented to the vehicle power and control designer was the typical one of meeting system specifications inside constraints of cost, ease of assembly, maintainability, and time to produce. The following sections treat the designer's approach in performing this task.

2.1 Determination of the System Power Requirements

Appendix A outlines the procedure followed in determining the power required to accelerate the vehicle at the amplitudes and frequencies called for by the specifications. An additional 100 pounds was added to the nominal vehicle weight for the purpose of calculating the required accelerating force. This figure represented an estimate of the additional pseudo loading due to wheel and bearing friction and drive system inertia, together with an allowance for future addition of dead weight to the nominal vehicle size.

The peak power requirement, corresponding to the case for constant acceleration over 16 feet of track, was determined to be 3.8 hp. The power requirements for sinusoidal motion of the sled, within the frequency and amplitude bounds set by the specifications, were all less than this figure.

Derivation of the power requirements for sinusoidal accelerations of the sled also produced the expression relating commanded acceleration to displacement amplitude and the frequency of oscillation:

$$\ddot{x}(t) = -X\omega^2 \sin \omega t \qquad (2.1)$$

The preceding equation shows that the sinusoidal frequency is related to the acceleration through X, the displacement magnitude. It is apparent that for the highest frequency specified ($\omega = 2\pi$ rad/sec), the cart need travel through only a few inches to achieve the specified acceleration amplitudes. For large accelerations, however, the cart must move through very large displacements if low frequency motions are desired.

Following the approximate power calculations, the control design problem was reduced to one of finding a drive system able to supply 3.8 hp over displacements ranging from a few inches to 32 feet. In addition, the desired system had to respond, when loaded, over a frequency range extending from zero to one cycle per second.

2.2 Mechanical Subsystem Design

The designers investigated several methods for transmitting the control power to drive the cart

A. Direct drive
B. Threaded shaft and nut
C. Hydraulic piston
D. Open wound induction motor
E. Winch, cable and pulley

The relative merits of the first four methods and the reasons why they were not employed in this application are briefly set forth in Appendix B. The designers settled on the winch, cable and pulley arrangement (see Figure 2). This transmission system appeared adaptable over the wide range of vehicle displacements called for by the specifications. It could be simply constructed from readily available materials. The designers were aware that the use of cable to join the load to the power source was tantamount to constructing a large spring-mass system and introducing a possible problem with high frequency oscillations.

Having settled upon a winch and cable drive, the next free variable to come under consideration was the diameter of the winch drum. A very large diameter drum was ruled out because of its attendant high inertia.

A very small diameter load drum was not employed for it would have had to operate at high angular speeds to move the load at the peak velocities called for through the acceleration specifications.

A load drum diameter of eight inches was chosen. A large factor in the decision was the availability of materials, namely pulleys, in this size range. Pulleys appeared adaptable to use as the winch drum member. Using eight inches as the load drum size, the speed and torque requirements at the load drum shaft were calculated for the constant and sinusoidal acceleration regimes. The reader is referred to Appendix C for the details of this calculation. It is sufficient to note here that the peak torque requirement amounted to 480 inch pounds and the peak speed reached 500 rpm. Note that in the case of sinusoidal acceleration, the peak torque and speed do not occur at the same instants in the acceleration cycle.

Design of the mechanical subsystem further narrowed the engineering task to one of finding a suitable source of rotary power. The source had to have a capability of 3.8 hp at 480 inch pounds and 500 rpm to satisfy the conditions for constant acceleration. For sinusoidal motions of the cart, the rotary power system would be called upon to submit to reversals of direction at least twice per second.

2.3 The Rotary Power Source

The driving system was envisioned as the signal to power transducer in a closed loop position controller. The block diagram of Figure 2a shows the location of the drive in the control loop.

Both an electric system and one employing high pressure

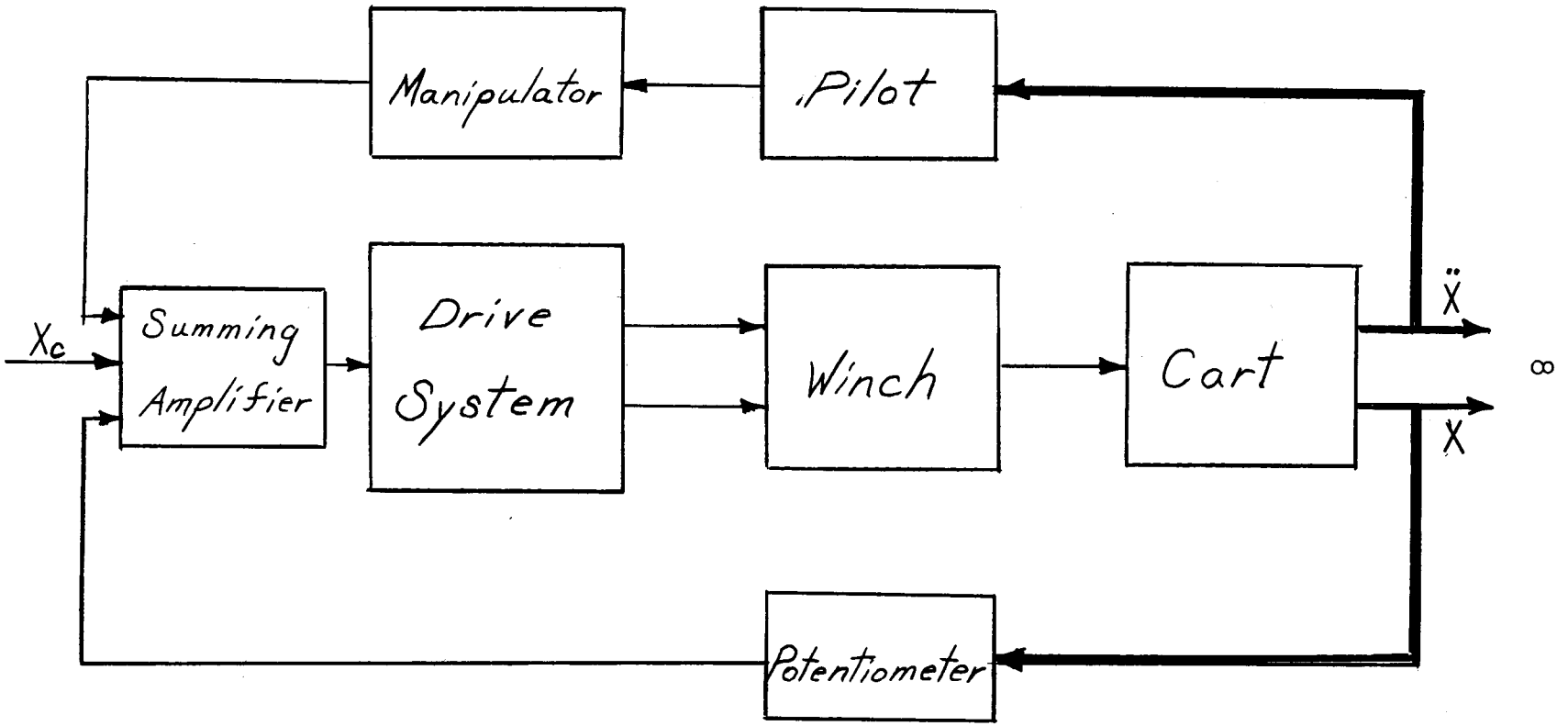

Figure 2.3a The general closed loop servo block diagram.

hydraulics were studied. Appendix D reviews the details of this study and contains a discussion of the relative merits of each system. A hydraulic rotary motor was chosen as the preferred method of driving the winch. The choice was made largely on the superior frequency response and high power outputs to be realized with a small hydraulic motor and valve. The necessity for handling messy and inflammable fluids was accepted as the chief drawback in this choice.

Figure 2 displays the block diagram for the hydraulic system that was ultimately assembled. The fluid circuit diagram appears in Appendix E.

High cost made impractical the assembly of this system from new hydraulic components. The hydraulic pump, valve, motor and the speed reducer were all secured as surplus or used components from sources available to the designers. As a result, the process of selecting an optimum drive became a problem of adapting given materials to meet the requirements at the winch drum shaft. The calculations involved are explained in Appendix E. The reader is referred to Figures 1, 2, 3 which depict the system assembled.

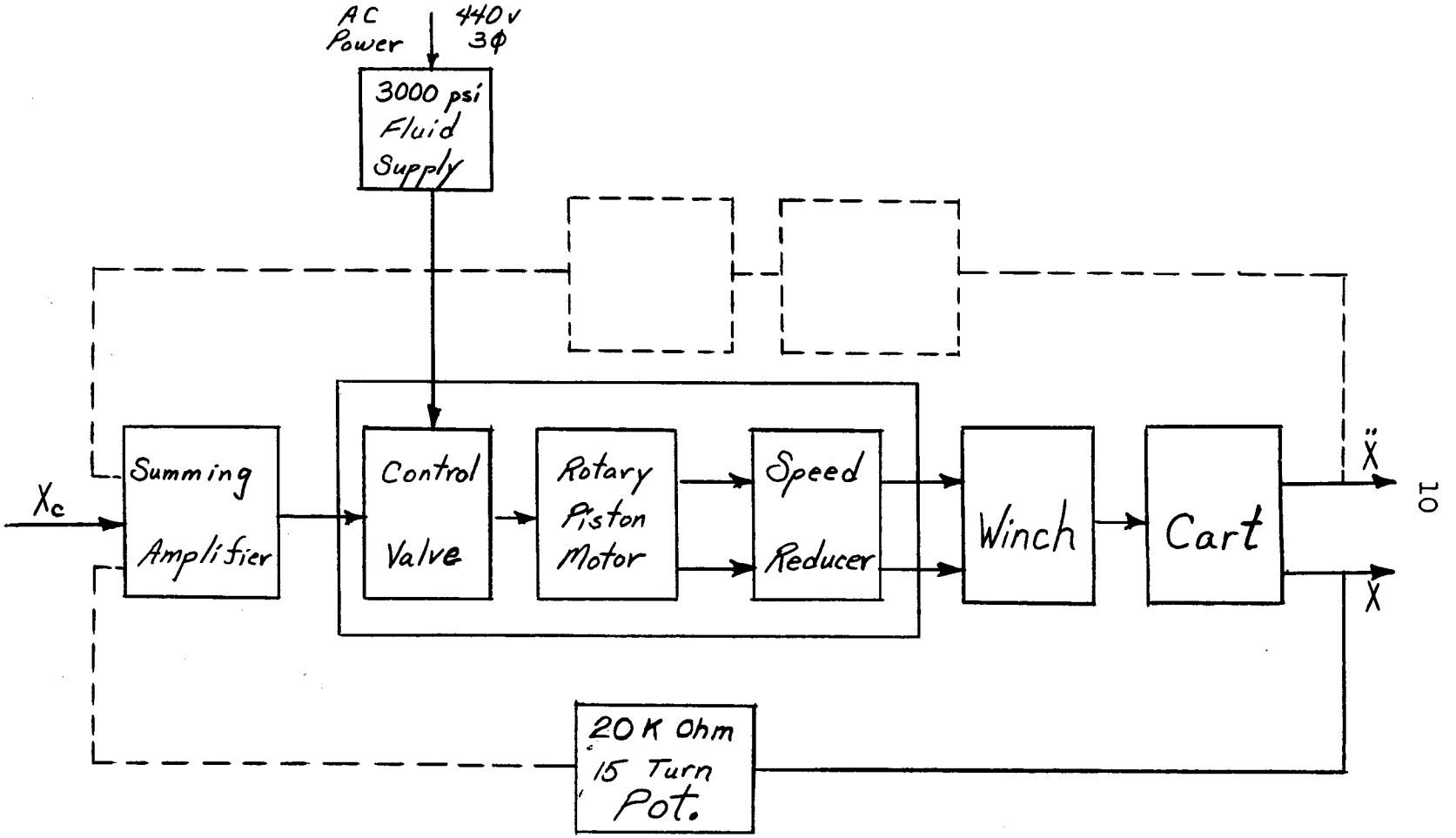

Figure 2.3b. The control system assembled to date

CHAPTER 3

Vehicle Design

3.1 The Vibration Problem

Elimination of transverse longitudinal and vertical vibrations above the threshold of .01g was the most difficult problem encountered in the design of the vehicle. Forced vibrations were determined to arise from three primary sources:

(a) Running surface deformities

(b) Wheel unbalance and eccentricity

(c) Wheel bearing chatter

In order to obtain an estimate of the scope of the problem, a sinusoidal vibratory waveform was assumed and the relationship between frequency and displacement amplitude plotted for an acceleration tolerance of .01g (See Appendix F). The result of this plot presents a fairly discouraging picture, since the vibratory amplitude varies inversely as the square of the frequency, and at frequencies above one cycle per second becomes exceedingly small. If now we look specifically at the running surface, and assume a completely rigid vehicle and a smooth running surface with a single bump on it, we find that the vertical accelerations now increase with the square of the vehicle's velocity:(4)

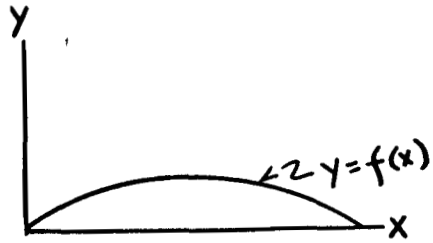

Let the bump be represented as $y = f(x)$. For a vehicle with speed V we have $x = vt$ and the vertical velocity is then:

$$\frac{dy}{dt} = V\frac{dy}{dx} \qquad (3.1)$$

The vertical acceleration becomes:

$$\frac{d^2y}{dt^2} = V^2\frac{d^2y}{dx^2} + \frac{dy}{dx}\frac{dV}{dt} \qquad (3.2)$$

For V ≠ constant. Thus the vertical acceleration varies both with the square of the vehicle speed and with the horizontal acceleration. If, for purposes of a simple preliminary examination, V is assumed to be constant, then the vertical acceleration becomes:

$$\frac{d^2y}{dt^2} = V^2\frac{d^2y}{dx^2} \qquad (3.3)$$

where $\frac{d^2y}{dx^2}$ is a property only of the shape of the bump, and for a bump of given shape the vertical acceleration varies as the square of the speed. If we assume a sinusoidal bump structure, then $y = Y \sin wx$, then the maximum vertical acceleration obtained in passing over the surface would be:

$$a_{MAX} = \left(V^2 \frac{d^2y}{dx^2}\right)_{MAX} \qquad (3.4)$$

or

$$a_{MAX} = \left(V^2_{MAX} \omega^2 Y\right) \qquad (3.5)$$

Here we find that for a periodic surface irregularity the maximum acceleration produced is not only dependent on the square of the speed, but the square of the frequency of occurrence as well (w being in units such as radians per inch). In other words, the shorter period of the surface waveform the greater the accelerations.

The results of wheel eccentricities upon the vibratory acceleration schedule were examined by assuming a single disturbance such as that produced by a single "lump" on a wheel (see Appendix F). The disturbance frequency was then calculated for various diameter wheels at maximum vehicle speed. This maximum frequency then would be the governing factor in determining the maximum allowable disturbance amplitude. Dual (or more) disturbances such as might be obtained from a slightly elliptical wheel, would simply produce the effect of increasing the frequency, and thus lowering the amount of eccentricity that could be tolerated. Bearing chatter was assumed to be of secondary importance, and could be overcome by the use of good quality bearings.

These initial estimates of the vibration problem led to

considerations of the proper wheel and suspension system for the vehicle, through which the excessive vibrations could be eliminated or absorbed.

3.2 The Suspension System

Possibly the most important result from the preliminary investigation of the vibration problem was a negative one, in that it was determined that there was really no way to predict the type, amplitude, or frequency of the disturbance (forcing function). Rough estimates could be determined from the maximum amplitude of the vertical displacements that could be expected, but waveform and frequency (other than the frequencies predicted as a function of wheel diameter and speed) remained totally unknown quantities. Initially a non-rigid suspension system, with or without damping, of the type most commonly encountered in automobiles was considered. This was discarded as presenting too many difficulties, and providing acceptable components (wheels, running surface, etc.) could be obtained, probably unnecessary. The most critical problem was that, in order to keep the natural frequency of the system well below the frequency of the forcing function (for maximum attenuation), the suspension would have to be extremely soft. For example, if the vibratory displacement, a function of the running surface, could be held to .1 inch, then any vibratory frequency above 1 cps would produce excessive accelerations. Since the natural frequency of a spring mass system $\omega_N = \sqrt{\frac{k}{m}}$, then in order to keep the natural frequency below 1 cps, say at .5 cps, the spring

constant K would have to be 1.94 lb/in, i.e.,

$$\omega_N = \sqrt{K/m} \qquad (3.6)$$

$$m = \frac{300^{\#}}{g} \text{ or } \frac{75^{\#}}{g} \text{ per wheel.}$$

$$\therefore \quad \omega_N = \sqrt{\frac{K}{75/g}} = .5 \times 2\pi$$

or

$$K = \frac{75\pi}{386} = 1.94\ ^{\#}/_{IN}$$

The softness of the suspension system would then produce problems of side-sway, pitch, and roll, as well as starting and stopping transients.

The decision to design for a rigid or near-rigid suspension system was reinforced by a trip to the Grumman Aircraft Corporation at Bethpage, Long Island. Grumman had a simulator in operation similar in principle to the designers' initial concepts. They had used a rigid suspension in conjunction with ordinary industrial casters, and were having no problem with vibration, using steel bar as the running surface. Hence it was decided to adhere to the formulated decision for a rigid suspension, or an extremely "stiff" suspension having a high natural frequency and high damping, in order to "isolate" the frame from high frequency vibrations where the disturbance amplitude tolerance is extremely small. Having decided on the type of suspension, it was necessary to find commercially available wheels that would produce acceptable results when employed with this type of suspension.

3.3 Selection of the Wheels

The possible alternatives here can be broken down into four possibilities:

(a) Metal wheels

(b) Hard rubber wheels

(c) Semi-pneumatic wheels (including natural rubber)

(d) Pneumatic wheels

Initial consideration was given to using metal wheels, running on metal rails (i.e., railroad type construction). After some consultation with the Boston Metropolitan Transit Authority, a piece of equipment was found which, it was thought, might be suitable. This was the Nolan Tool and Supply Cart, a 48" x 45" tubular steel cart weighing 140 pounds and running on cast steel wheels. However, after locating one of these units and test riding it, it was determined that an unacceptable amount of vibration existed due primarily to the crude construction of the wheels and bearings, and secondarily to the irregular rail surface. Thus the "railroad" approach per se was discarded, and other possible solutions investigated. An automotive type wheel and axle system was considered next using pneumatic tires. This system presented the advantages of excellent bearings, (Timken tapered roller bearings in most cases), an available "platform" on which to mount a suspension system, should one later be required, and pneumatic tires which would (a) deform slightly under load to counter the eccentricity problem, and (b) act as a stiff spring to isolate the frame somewhat from shock and high frequency vibration. However, the overriding disadvantage of this system was the weight. The lightest wheel and axle configuration

that could be located commercially weighed 55 pounds. Thus two sets would weigh 110 pounds or ten pounds over the initial desired weight for the entire vehicle. It was at this point that the trip to Grumman mentioned earlier opened up the possibility of using commercially available casters. Although Grumman had used metal casters surfaced with hard rubber, it was decided, if possible, to use something somewhat more resilient to provide some of the advantages described above of pneumatic tires. In addition, B.S. Cain in his book "Vibration of Rail and Road Vehicles" had presented some data from vibration experiments which were conducted with streetcars using different types of wheels.(2) These experiments demonstrated conclusively that rubber tired wheels produced far lower vibratory accelerations when running on metal track than any metal wheel tested. The reason they are not employed on this type of vehicle is due to tire wear, which in this project was not a critical factor. Thus the wheel finally decided upon was the Lauco Balloon Wheel, manufactured by the Charles P. Lauman Company in Boston. These wheels provide a two-inch tread thickness of natural rubber, with good resilience weighing only seven pounds each. The natural rubber represents a promising compromise between the metal or hard rubber tread and the pneumatic tire, with a substantial reduction in weight over the automotive type wheel. Pneumatic and semipneumatic caster assemblies were also available, but they seemed to present no advantages over the natural rubber tread. The pneumatic casters were generally heavier than the Lauco Wheels and could not be obtained in a smooth tread. The semipneumatic casters were also generally

heavier and had lower quality bearings. The Lauco Wheels obtain their reduction in weight through the use of a cast aluminum hub and wheel.

Other considerations beside weight and resilience governed the final selection. Although the bearings in the Lauco Wheels are only of industrial quality (unmachined race) they can if necessary be pressed out and precision bearings installed. There is also enough material in the hubs to permit them to be milled out slightly for the installation of a larger diameter bearing, in case precision bearings of the same diameter as the ones presently installed could not be found. The deflection of the tread under load eliminates the necessity of shimming the wheels to insure that all four touch in the same plane that would be necessary in the case of hard rubber or metal wheels. The hubs and axles are drilled and fitted for lubrication, a factor which was found on few other casters, and last but not least, the price per assembly was very reasonable.

The wheel selected was 8 inches in diameter. This size was selected as a compromise between two factors. It has been shown that a larger wheel would be able to tolerate a larger eccentricity or unbalance due to its lower frequencies at a given velocity. Opposed to this was (a) a desire to keep the center of gravity of the vehicle as low as possible for stability purposes, and (b) the rapid increase in weight and caster plate size with each increment of increase in wheel diameter. It was felt that the 8 inch wheel represented a good trade-off between these opposing factors. It

might have been possible to use a smaller wheel, since disturbance amplitude tolerance for a single irregularity varied only .005 inches for an 8 inch change in diameter.

3.4 The Running Surface

Proceeding concurrently with the selection of the type of suspension system and the type of wheel to use, was the problem of reducing running surface deformaties. As was mentioned before, rails were initially considered, but were rejected primarily because an acceptable wheel could not be found to employ with them. The surface in the laboratory building is concrete, from 12 to 18 inches thick and in generally good condition, although rough spots do exist. It was felt that a smoother more regular surface would be needed, and it was originally planned to run the wheels over two tracks formed by bolting cold rolled steel bar stock to the concrete. The cold finished steel surface would be extremely smooth and the bars could be shimmed to insure a level surface. However, since the concrete was in fairly good condition, and due to a reasonable question of the necessity of doing this, it was decided to assemble the vehicle and test it on the concrete using vibration pick ups before making a final decision to use steel track.

3.5 Carriage Design

The selection of the wheel assemblies determined one design parameter for the carriage. That is—the carriage had to have a structural member wide enough to mount the

caster bracket. Other design criteria were:

(a) Strength and rigidity

(b) Weight

(c) Cost

(d) Ease of construction

(e) Flexibility in design, leaving room for possible future modifications

(f) Stability, for all positions of the test subject

The carriage is five feet square. Since the subject is to be rotated through 360° during various experiments, the square was the obvious choice for the geometrical shape of the vehicle (other than a quite impractical circle). The five foot dimension was determined by both safety and stability considerations with the subject in a prone position. A six foot individual in this position will project only six inches over the sides of the carriage during a run, affording him the full protection of the frame in almost all other positions, and preventing any tendency to tip due to the shift of the subject's center of gravity in various positions (Fig. 5).

The frame is entirely of bolted construction. Welding was avoided in order that the carriage could be easily disassembled if future modification is required. The frame is also easily adaptable to a different type of caster, and can also be fitted to axles without much difficulty.

Aluminum was selected for the material for strength, rigidity and low weight. Specifically the main structure

was constructed out of 60 61-T6 structural aluminum angle and "U" channel. The size of the angle, 3 x 4 inches, was determined by the width of the caster plate which required a four inch flange. This in turn determined both the size of the other leg (three inches) and the thickness (one-quarter inch), due to the fact that these dimensions represent the minimum dimensions available in a standard aluminum structural angle with a four inch leg. The shapes selected, angle and "U" channel, were chosen for rigidity in bending. The "U" channel selected for the cross braces was 4" x 2" x 1/4" 6061-T6 structural aluminum channel. Deflection computations were made for maximum loading conditions (see Appendix G), and the resulting deflections were considered to be acceptable. The natural frequency under load for these structural members were also computed (see Appendix G), and were considered acceptable from the standpoint that they were well above the maximum characteristic frequency of the wheels. The maximum deflection of the main structural members (angle) was computed to be .0415 inches, and for the cross members ("U" channel) .0304 inches. The computed natural frequencies were 15.3 cps and 18 cps, respectively.

A 1/4 inch 6061-T6 aluminum plate, 24" x 24", was placed at the center of the vehicle supported by the cross braces in order to (a) provide a support for the swivel mounted chair assembly, (b) assist in distributing the load to the cross braces, and (c) to provide resistance to torsion. Additional torsional rigidity was provided by the use of 1/4 inch

aluminum gussett plates in joining the structural angle together at the corners. However, the major resistance to torsion is provided by the chair platform as will be discussed later.

In order to complement the resilient vibration absorbing qualities of the wheels, the casters were shielded from direct contact with the frame by means of 1 inch thick rubber "sandwiches" (Fig. 7). The mounting bolts were also insulated by means of rubber bushings and washers, so that there was no metal-to-metal contact between the frame and the casters. Since rubber springs absorb energy, and rubber effectively damps out high frequency vibrations, the use of rubber pads is in keeping with the vibration "isolation" concept of the suspension.

3.6 The Chair Assembly

Two major considerations governed the design of the chair.

(a) The initial specifications which required the subject to be placed in any position from 90° sitting to prone, and from 0° to 360° to the direction of motion

(b) Weight

The chair selected was an ordinary tubular aluminum lawn chair of the "chaise lounge" type. The tubular aluminum construction provided light weight, and the chair could be raised and lowered through almost the full required range of positions. Furthermore, the webbing provides additional insulation against vibration. However, two modifications

were necessary before the chair could be used. First, although light weight, the chair was not rigid enough and exhibited a pronounced tendency to sway. Thus it was necessary to provide extra bracing for the chair to increase its rigidity. The bracing used can be easily seen in Fig. 4 Secondly, it was necessary to modify the positioning plates on the chair arms so that an almost continuous selection of positions from prone to 90° sitting was available.

The chair was mounted by rubber insulated conduit clamps to a 4' x 5' section of 3/4 inch plywood. Wood, as opposed to metal, was chosen as the material to minimize the transmission of vibration from the carriage to the chair, and the thickness was selected to provide a secure foundation both for the mounting of the chair and also for the mounting of seat belts. The wood platform is pivoted about a 3/4" steel bolt tapped into the center plate of the frame by means of a copper bushing pressed into the wood. The chair platform is held to the frame by means of this center bolt and by "C" clamps. The use of the clamps provides a simple method of locking the chair in any position to the line of motion from 0 to 360°. The chair platform, when clamped to the carriage, provides the principal resistance to any torsional moments applied to the assembly.

3.7 The Guide Vanes

Once the basic design of the cart was decided upon, several methods of assuring straight line motion were considered. The principal ones were:

(a) Running the wheels in "U" channel or in the "V" of a structural angle

(b) The use of spring loaded wheels or bearings running against a track on each side

(c) Low friction runners on a guide rail

The first method was rejected since it was felt that the "U" channel would permit too much clearance between the side of the tire and the flange of the channel, allowing the vehicle's wheels to slip from side to side of the channel as the vehicle passed down the track. This would cause unacceptable transverse oscillations. The structural angle idea was discarded since it was felt the "V" might pinch the rubber tread, and retard the motion of the vehicle.

A considerable amount of serious thought was given to the use of spring loaded wheels. However, this system seemed to introduce the same problems in the guidance that we were trying to overcome in the basic vehicle design. Specifically, it would introduce problems of bearing chatter, eccentricity, and to a lesser extent running surface smoothness. Hence, this idea was eventually discarded as well.

The final system selected depends upon the employment of the abhesive qualities of teflon, and is quite a bit simpler than the before mentioned system. The guidance is provided by use of two pairs of teflon block (3" x 1" x 1/2") runners mounted at each end of the vehicle by means of aluminum vanes. Each pair of runners straddles a guide rail, running the length of the test bed. The clearance between the runners and the rail can be adjusted by means of set screws, so that the runners can be clamped to the

rail, and backed off just enough to permit the vehicle to slide freely down the rail. The rail, itself was manufactured from 2 1/2" x 1/2" cold rolled steel bars, butted together to form a smooth surfaced 40 foot guide rail, and mounted to the concrete floor every two feet by brackets cut from 2" x 2" x 1/4" structural steel angle. The brackets clamp the rail in a vertical position allowing 1 1/2 inches to project above them for a running surface. Although the runners are only one inch wide, the extra 1/2 inch of rail allows different deflections of the vehicle wheels under varying loads. The teflon runners are backed by 1/8 inch aluminum plate in order that the load on the attaching bolts be taken primarily by the tapped holes in the aluminum rather than the threads tapped into the comparatively soft teflon (Fig. 6).

3.7 Mechanical Safety Devices

Two mechanical safety devices have been designed to protect the test subject against a malfunction of the control system. Aircraft type seat belts and shoulder harnesses have been installed on the vehicle. The belts and harnesses are mounted to the plywood platform by means of eye-bolts. The second safety device is an arresting gear which will be installed at each end of the run. Computations were made to determine the necessary stopping force required to bring the vehicle to a halt in various distances if the vehicle were running at the maximum velocity of 16 fps (see Appendix H). Each arresting gear consists of four strips of 5/8 inch

and two strips of 1/2 inch "bungee" cord. These strips will be one foot long and at 100 per cent elongation will provide 1790 pounds of stopping force or a 4.5'g deceleration if the vehicle hits the barrier at peak velocity. The 100 per cent elongation will allow the vehicle to be stopped within the required one foot distance, and provide a 40 per cent safety factor since the ultimate breaking strength of the bungee is at approximately 140 per cent elongation. This amounts to a 90 per cent increase in load capability at 125 per cent elongation. The bungee cords will be attached at one end to 3/4" bolts in the concrete floor, and will be tied together at the opposite ends by 3/16 aircraft cable (breaking strength 3700 pounds). If the vehicle goes past the maximum allowed run, the cable engages the aluminum guide vanes and the bungee cord will bring the vehicle to a stop. No provision was made to install a device to lock the vehicle in place after it is brought to a stop, since it is attached to the drive system at both ends by cable, and in order to "snap" back in the opposite direction would have to overcome the hydraulic motor and reverse it, a situation considered unlikely. If this should happen, the motor and pulley system should provide adequate resistance or "drag" so that the bungee tension should be reduced gradually.

Additional electric safety devices will be provided to complement the mechanical safety features. These are in order of occurrence:

(a) A power reversal mechanism to drive the motor in the opposite direction if the vehicle exceeds the maximum allowable run

(b) A power cut-out to shut off power to the system completely if the reversal mechanism fails.

CHAPTER 4

TEST RESULTS AND CONCLUSIONS

4.1 Introduction

Figure 2.3b is a functional block diagram of the power and control system constructed and tested by the designers. Complete closed loop operation had not been achieved prior to the completion of this thesis but open loop tests were conducted to verify that the mechanical performance was adequate. These tests also offered some indication of the control performance to be expected. The test procedures and results are described in the following sections.

4.2 Test Procedure

The first tests on the completed cart-motor system were designed to verify that the collection of used and surplus equipment would, indeed, operate.

The pump was tested by operating with the high pressure port connected directly to the reservoir. Zero pressure flow was maintained for 30 minutes to filter the oil and clean the hydraulic lines.

Next, the pump was connected directly to the ports of the hydraulic motor. The cable joining the winch to the vehicle was removed and the designers proceeded to test the compatability of the hydraulic motor, the speed reducer and the winch. Unidirectional oil flow was maintained through the motor at a system pressure of 500 psi, while the tube and hose fittings were checked for leaks. None were found. (None were expected at this low pressure.)

The third step in the test sequence was conducted with the cart still disconnected from the winch. The tube and fittings joining the valve manifold to the motor were assembled, the high pressure and return lines from the pump were connected to the manifold ports, and the servo valve was placed on the manifold seat. Prior to starting the pump, the filter element in the high pressure line was replaced.

The Moog servo valve (Model 2004A) discussed in appendix E was employed in the initial testing. This valve failed during the course of the sinusoidal tests and was replaced with Moog valve Model 1803. All system tests were then redone for the new valve.

At an operating pressure of 1200 psi, the line fittings were again checked for leaks and the valve was mechanically centered to stop motor rotation. The valve was then subjected to step input of current at plus and minus 5 milliamps. No higher pressures were attempted since reversing the unloaded drive system sent high pressure transients back to the pump. These transients were within 1000 psi of the maximum hose pressure rating of 3500 psi.

Next, the cart was connected to the winch by taking two turns of the winch cable around the winch drum. The cart was loaded with 160 pounds of sand and the step input tests were repeated. The loading of the power system damped the high pressure line surges to plus and minus 200 psi about the operating pressure of 1500 psi.

Finally, a d-c amplifier and a low frequency oscillator were introduced in the control circuit preceding the valve. Figure 4.2a displays the block diagram of the electrical circuit.

The cart, operating under a 160 pound load, was subjected to sinusoidal accelerations of constant amplitude at frequencies of .33, .5, 1, 2, and 3 cycles per second.

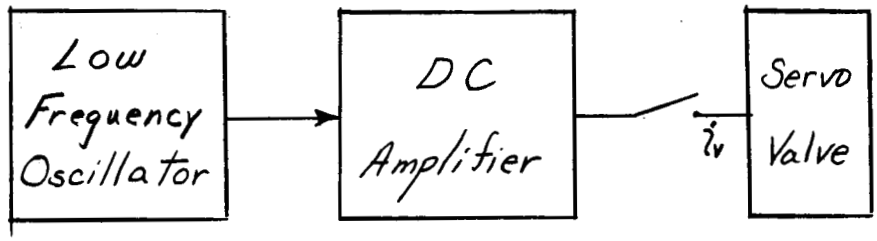

Figure 4.2a. A block diagram of the oscillator circuit driving the valve.

Lower frequencies were not tested because of drift in the amplifier which produced uncontrollable motions of the sled at low frequencies. Higher frequency information was deemed unnecessary.

A 20 thousand ohm, 15 turn potentiometer mounted on the winch shaft was excited with a 12 volt battery and used to give an indication of vehicle position on the track. Both the amplifier output signal and the potentiometer reading were recorded on a dual channel oscillograph recorder.

4.3 Analysis of Results

The steps preceding the frequency response investigation generated no numerical data. The pump, hydraulic motor, speed reducer and all the associated fittings were shown to be operable and capable of moving the loaded vehicle in response to step inputs of large magnitude. The cable joining the winch drum to the cart was observed to be binding on the winch support channel. This defect was corrected by modification of the support member.

The data derived during sinusoidal tests of the loaded vehicle is displayed in Appendix I. Reduction of the tape data led to the Bode plots of log (AR) and phase versus frequency shown in Graph I-1.

Examination of Graph I-1 indicated that the response of

the loaded vehicle to an input signal of constant amplitude but varying frequency was slow. The linear performance function for a valve-motor combination under constant pressure should, ideally, be of the form

$$(PF)_{s(i,\theta)} = \frac{K}{\delta\left[1 + \frac{2\xi}{\omega_n}s + \frac{s^2}{\omega_n^2}\right]} \qquad (4.1)$$

when the delays in the electrical valve circuit are neglected.[5] The sinusoidal response of a system with this performance function should lead to a Bode plot of the form given in Figure 4.3a.

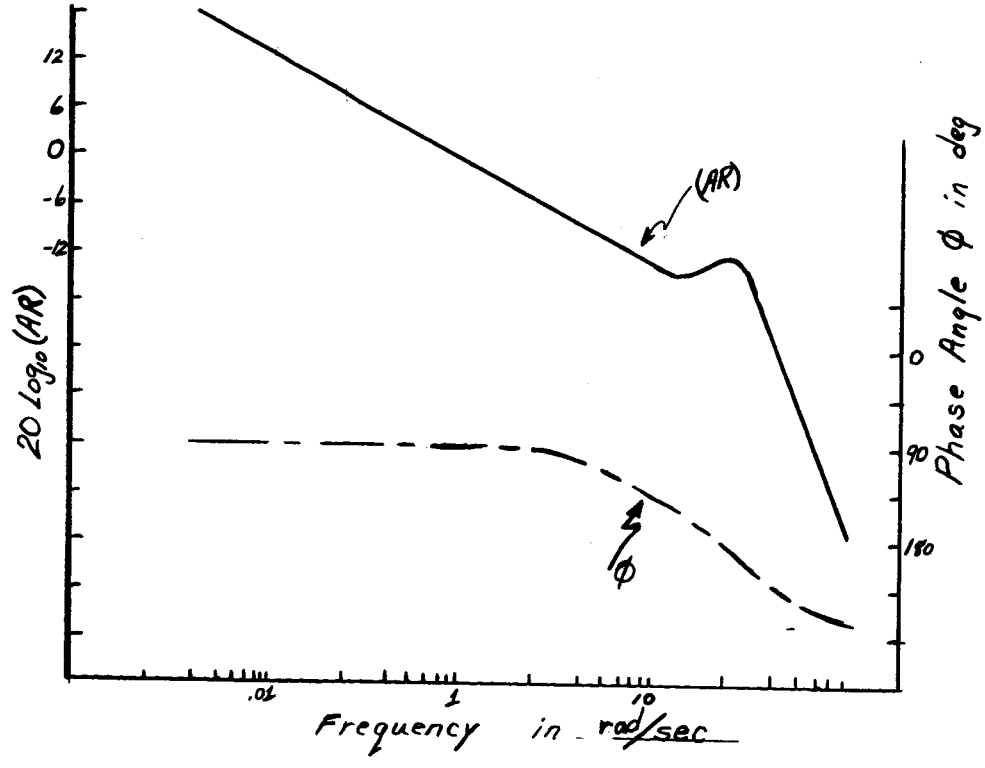

Figure 4.3a. A Bode plot of log (AR) and phase versus frequency for the ideal valve-motor performance function.

At low frequencies (0 → 1 cps), the $\log_{10}(AR)$ should be decreasing at 6 decibels per octave. The natural frequency, ω_n, of the second order mode should have a value on the

order of 2 cycles per second for this application.

The observed performance of the open loop system did not correspond to the ideal performance function. Over the range of frequencies measured in the test (.3→3 cps), the $\log_{10}(AR)$ decreased at 12 decibels per octave. The Bode plot of Graph I.3 suggests that the actual performance function was probably more like

$$(PF)_{s(i,\theta)} = \frac{K}{s(1+s)(1+\tau_1 s)} \qquad (4.2)$$

The system appeared to suffer from over-damping with the second-order mode degenerating to two poles on the real axis in the complex plane.

Operation as described by the last performance function will probably not be acceptable when closed loop operation is attempted. Figure 4.3b shows the expected, uncompensated root locus for the tested system.

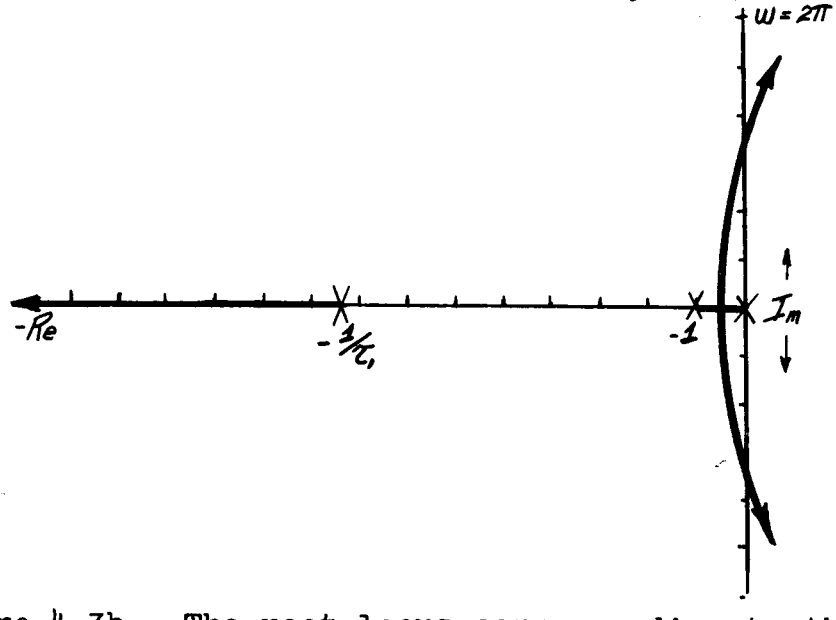

Figure 4.3b. The root locus corresponding to the observed open loop system performance function.

Instability can be expected for gains high enough to meet the frequency response requirements. Compensation could be added to stabilize the system but the designers suggest a more direct attack.

4.4 Suggested System Modifications

The first step to be taken toward improvement of the control and power system is introduction of a valve of higher flow rate. The designers used the Model 1803 Moog valve with full knowledge that its low flow rate could never sustain the high acceleration, low frequency trials called for in the specifications. The sinusoidal frequency tests suggest that the valve is also unable to adequately deliver the flow rates called for at low accelerations and high frequency. Appendix E should be consulted to find the proper flow rate when a new valve is ordered.

The hydraulic supply, as now configured, contains no accumulator. The high pressure transient surges now experienced at the supply when the vehicle direction is reversed could be cushioned and reduced by introduction of a 3000 psi accumulator bottle in the high pressure line. The operating pressure could then be safely raised to the design pressure of 3000 psi.

A constant pressure, valve controlled hydraulic system is notoriously inefficient.[5] In this system the lack of efficiency is manifested by heating of the hydraulic fluid. Heating leads to decreases in the density and bulk modulus of the oil. In turn, the natural frequency of the system's second-order mode is reduced. Heating may also lead to deterioration of the hose lines. Recommended operating temperatures lie between 160° and 200° F. The present system is operating without benefit of an oil cooler. The designers suggest that, at minimum, a temperature gauge be installed in the reservoir. If excessive oil temperatures are observed, a water jacket should

be wrapped around the oil tank.

The hydraulic circuit diagram of Figure E-6a shows a filter in the high pressure line between the pump and the valve. This filter is presently equipped with a 39 micron element. It is good servo practice to protect the servo valve with oil filters which capture foreign particles of size greater than 10 microns. Further system modifications should include the change from 39 to 10 micron filter elements.

4.6 Vibration Analysis

During the period from the time the construction and installation was completed until this report was due for publication, the designer's efforts were directed toward the "checkout" of the power and control system. Hence, quantitative data on vehicle vibration was not obtained. However, it was noticed by riding on the vehicle during the control tests that some residual vibration was being transmitted to the chair assembly. The amplitude and frequency remain quantitatively undetermined but it appears to be of fairly low amplitude and high frequency. The designers feel that the principal cause for this is the irregularities in the concrete floor. If future tests prove the acceleration level of these vibrations to be unacceptable, the installation of steel tracks as a running surface (as discussed in Chapter 3) will eliminate most if not all of these vibrations. The following process is suggested to reduce the vibration level, with tests being run at the end of each step to determine the necessity for proceeding further:

(a) Installation of cold rolled steel bars as a running surface for the wheels.

(b) Installation of shock mountings between the wooden platform and the chair (providing the residual vibration is fairly high frequency, i.e.,

above 20 cycles per second).

(c) Installation of precision bearings in the wheels.

LIST OF SYMBOLS

x = linear displacement in feet measured from the defined zero position of the cart to the centerline of the cart. For the case of constant acceleration, the zero position is taken at the end of the track. For sinusoidal accelerations, the zero position is arbitrarily defined at the center of the track.

$\dot{x}$ = the time derivative of displacement or the velocity.

$\ddot{x}$ = the second time derivative of displacement or the acceleration.

t = time in seconds

ω = frequency of oscillation in radians per second

m_s = mass of the sled in slugs

g = earth's gravity constant

F = the accelerating force in pounds

ρ = the instantaneous power

W = the work done on a system

X = the peak displacement amplitude

θ_L = the displacement of the winch drum in radians measured from an arbitrary reference

T_L = the torque applied to the winch drum shaft

T_m = the motor output torque

θ_m = the motor shaft's angular displacement in radians measured from an arbitrary reference

f = frequency in cps

E = modulus of elasticity

APPENDIX A

CALCULATION OF THE POWER REQUIRED TO ACCELERATE A 400 POUND MASS

A-1 Case for Constant Acceleration

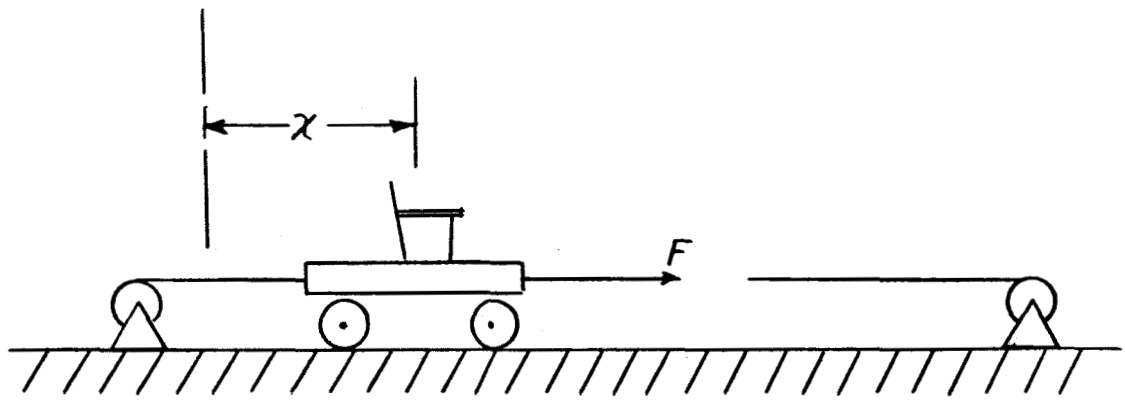

Figure A-1a Notation Convention for a Constant Applied Force F.

Visualization of the cart motion in response to a constant applied force is best achieved by considering Figure A-1a.

The displacement is measured from a null position at the end of the run. Assume the sled starts from initial conditions:

$$x = 0 \quad ; \qquad \dot{x} = 0 \tag{A.1}$$

The power required to give the sled a constant acceleration will reach a maximum when the sled velocity is maximum.

$$p(t) = F\dot{x}(t) \tag{A.2}$$

The point of maximum sled velocity will occur at mid-track if, at that point, the direction of the applied force is changed to decelerate the vehicle. The deceleration is applied to satisfy the safety requirement of zero velocity at x = 32 feet.

Figures A-1b, c, d, e display, respectively, the idealized

acceleration, velocity, displacement and instantaneous power associated with the vehicle motion over the full 32 feet assuming only one change in the direction of the applied force.

The maximum power requirement pertains for the maximum acceleration specified:

$$\ddot{x}(t) = a_1 = 9.66 \text{ ft/sec}^2 \qquad (A.3)$$

$$m_s = 12.4 \text{ s/ugs}$$

$$F = 120 \text{ pounds}$$

$$t_1 = 1.8 \text{ seconds}$$

$$x(t_1) = 16 \text{ feet}$$

$$\dot{x}(t_1) = 17.3 \text{ ft/sec}$$

$$\boxed{p(t_1) = p(t)_{max} = 38 \text{ hp}}$$

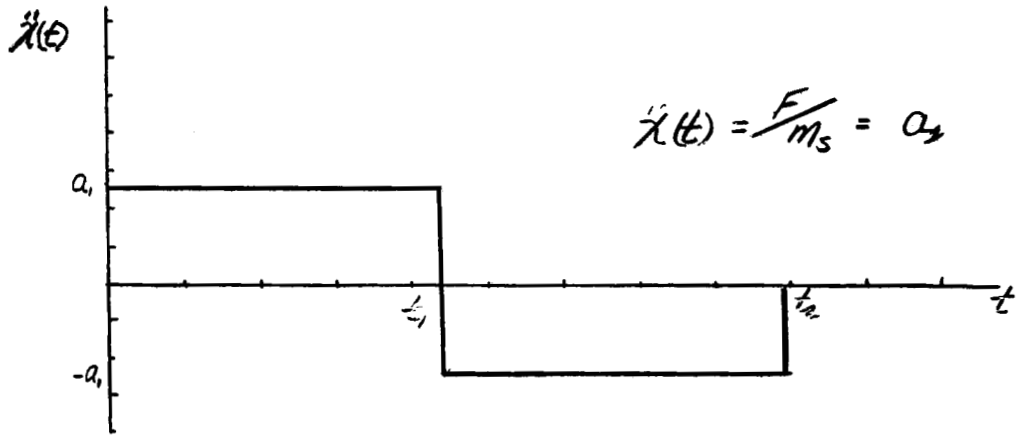

Fig. A-1b. Acceleration Profile vs Time.

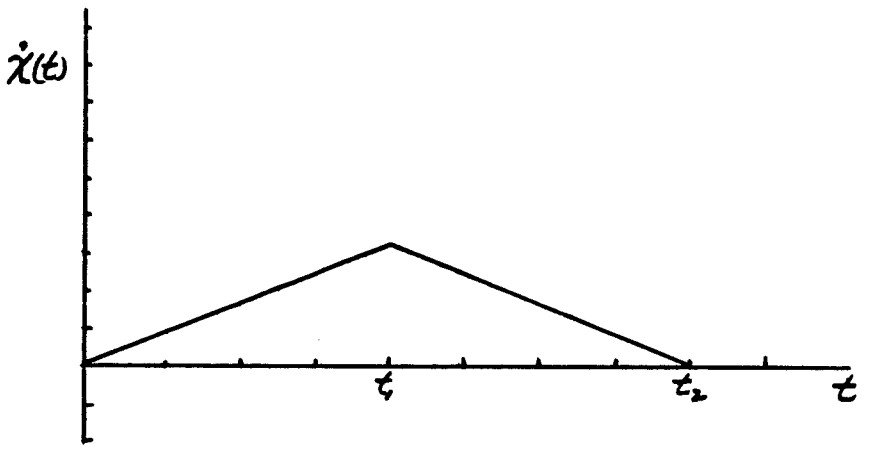

$$\dot{x}(t) = a_1 t + b$$

Fig. A-1c. Velocity Profile vs Time.

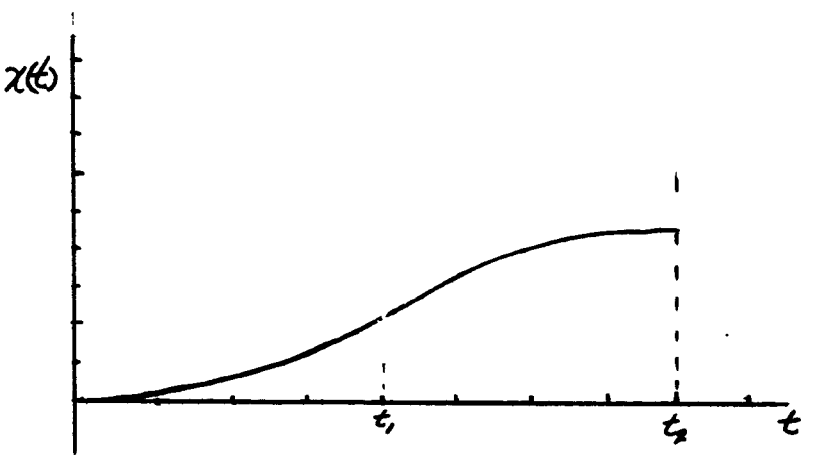

$$x(t) = \tfrac{1}{2} a_1 t^2 + b_1 t + c$$

Fig. A-1d. Displacement Profile vs Time.

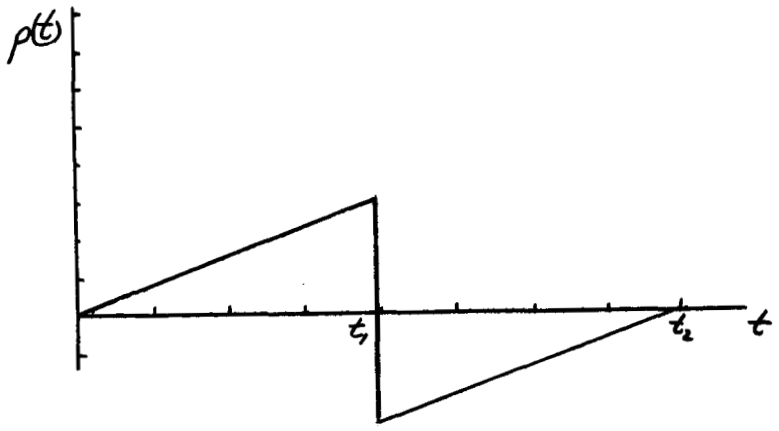

$$p(t) = F\dot{x}(t)$$

Fig. A-1e. Instantaneous Power vs Time.

A-2. The Case for Sinusoidal Accelerations

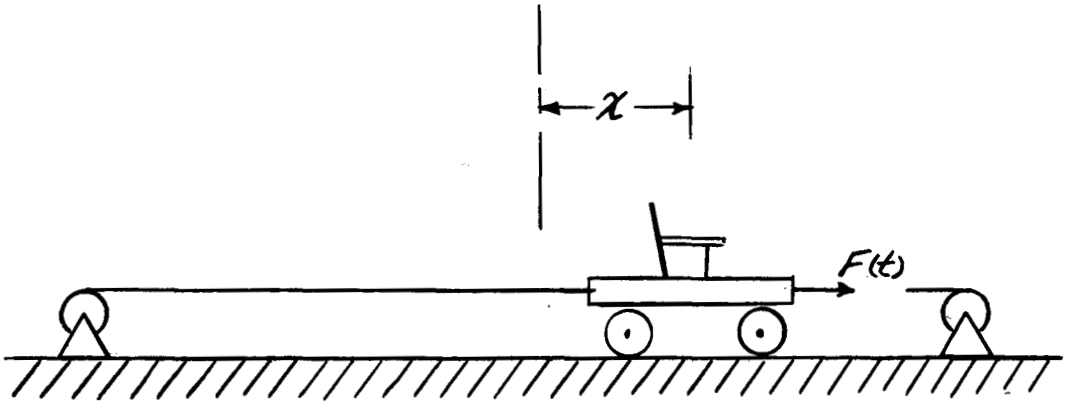

Fig. A-2a. Notation Convention for a Sinusoidal Accelerating Force F.

Visualization of the sinusoidal cart motions is enhanced by translating the displacement null from the end to the center of the run as indicated in Fig. A-2a. Now, negative displacements are possible and correspond to the cart occupying a position to the left of the track center.

The power required to force the cart into sinusoidal motions about the null position is given by the time derivative of the

work done on the cart by the accelerating force.

$$\frac{d}{dt}(W) = \frac{d}{dt}\left[\int F(t)dx\right] = \frac{d}{dt}\left[\int F(t)\frac{dx}{dt}dt\right] = F(t)\dot{x}(t) \qquad (A.4)$$

If a sinusoidal accelerating force is applied to the cart, assume it has the form

$$\frac{F(t)}{m_s} = \ddot{x}(t) = -X\omega^2 \sin \omega t \qquad (A.5)$$

then

$$\dot{x}(t) = X\omega \cos \omega t \qquad (A.6)$$

and

$$x(t) = X \sin \omega t \qquad (A.7)$$

where X is the magnitude of the peak displacement of the cart from the null position.

In this design problem, where $\ddot{x}(t)$ had a peak amplitude set by the specifications, X and w were functions of the acceleration. Note, for example, that at the upper acceleration limit of .3g's, the maximum available displacement, X = 16 feet, determines the minimum frequency which can be attained:

$$\omega_{min} = .776 \ \text{rad/sec} \qquad (A.8)$$

Figures A-2b, c, d, e display, respectively, the waveforms of acceleration, velocity, displacement and power associated with commanded sinusoidal accelerations of the sled.

The frequency, peak displacement and power required to attain the high and low sinusoidal acceleration magnitudes are tabulated in Fig. A-2f below.

Acceleration Amplitude $X\omega^2$ (ft/sec^2)	Radian Frequency ω (rad/sec)	Displacement Amplitude X (feet)	Peak Power Amplitude $\frac{1}{2}m_s X^2\omega^3$ (hp)
9.66	.776	16.0	1.34
9.66	2π	.245	.162
.322	.142	16.0	.008
.322	2π	.008	.0002

Fig. A-2f. The Displacement, Frequencies and Power Requirements for Sinusoidal Motion at .3g's and .01g's.

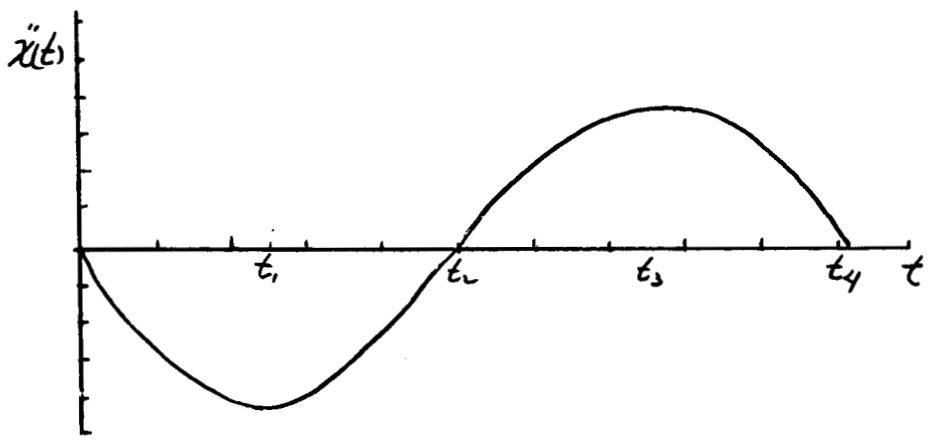

$$\ddot{x}(t) = -X\omega^2 \sin \omega t$$

Fig. A-2b. Acceleration profile vs time.

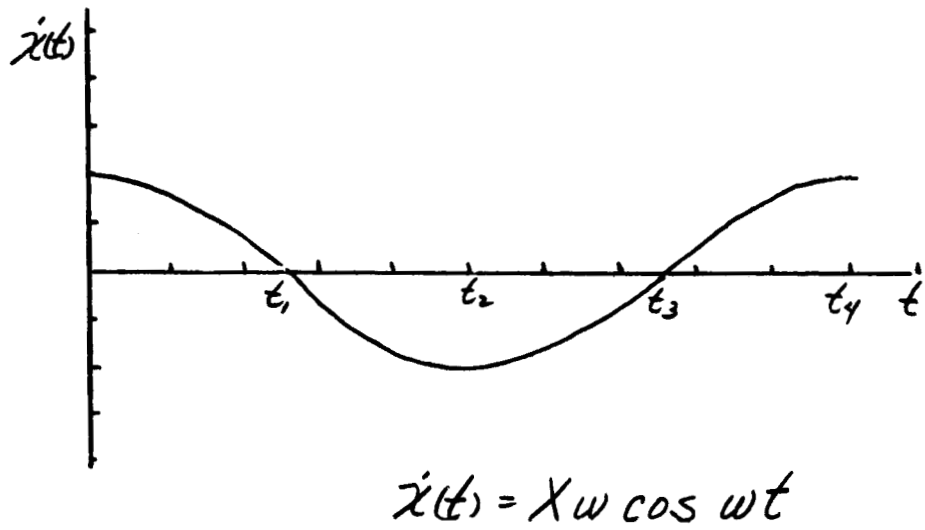

Fig. A-2c. Velocity profile vs time.

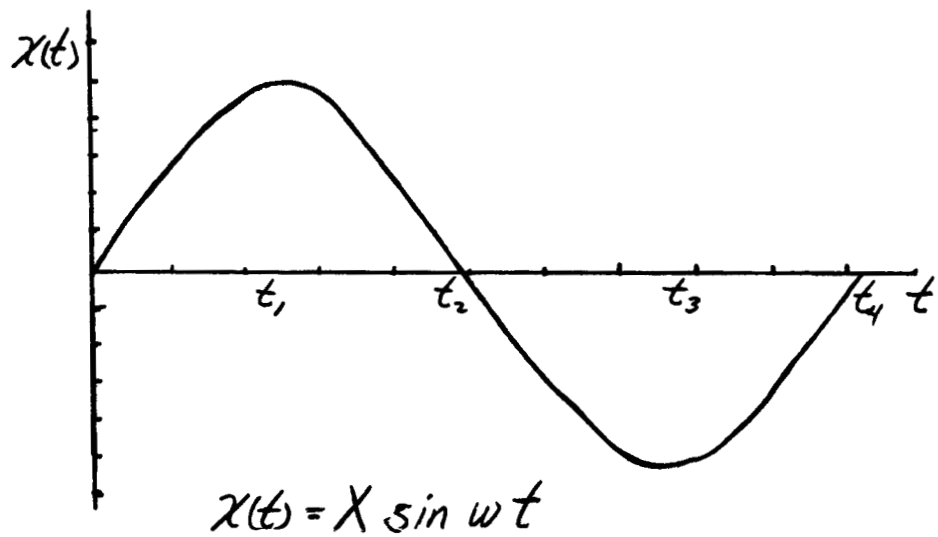

Fig. A-2d. Displacement profile vs time.

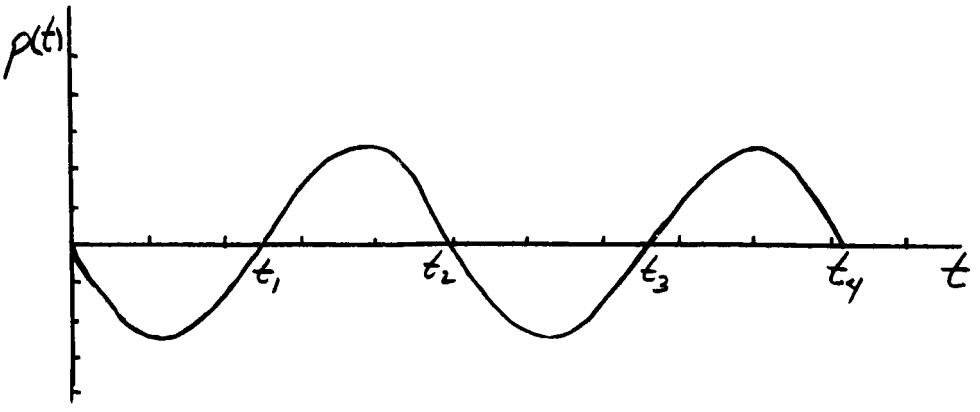

$$p(t) = F(t)\dot{x}(t) = -\tfrac{1}{2} m_s X^2 \omega^3 \sin 2\omega t$$

Fig. A-3e. Instantaneous power vs time.

APPENDIX B

COMPARISON OF METHODS FOR CONTROL POWER TRANSMISSION

The designers studied 5 methods for transmission of the control power required to move the cart. A winch, cable and pulley arrangement were employed in the assembled system but the merits of the other drives are discussed here in justification of the final decision.

B-1 Direct Drive

Initial study led the designers to a proposal for mounting the power source directly on the vehicle with a chain or fluid transmission between the motor and the wheels. In effect, this direct drive would have involved construction of a poor man's automobile. The system appeared compact and adaptable to the wide range of displacements.

The direct drive transmission was not employed for two reasons. First, the weight of an electric motor and gear train capable of delivering 4 hp was found to be 150 pounds. This weight would have overloaded the cart, required far greater accelerating power, a larger motor and thus more weight. Utilization of a light weight hydraulic motor could have been the solution to the weight problem. The second drawback, however, negated this suggestion. The designers could discover no practical method for conducting 3000 psi hydraulic fluid from a stationary pump to a motor oscillating through displacements as large as 32 feet. The designers were also concerned about vibrations which the motor might induce in the cart.

B-2 Threaded Shaft and Nut

Figure B-2a depicts the mechanical features of a shaft-nut drive system.

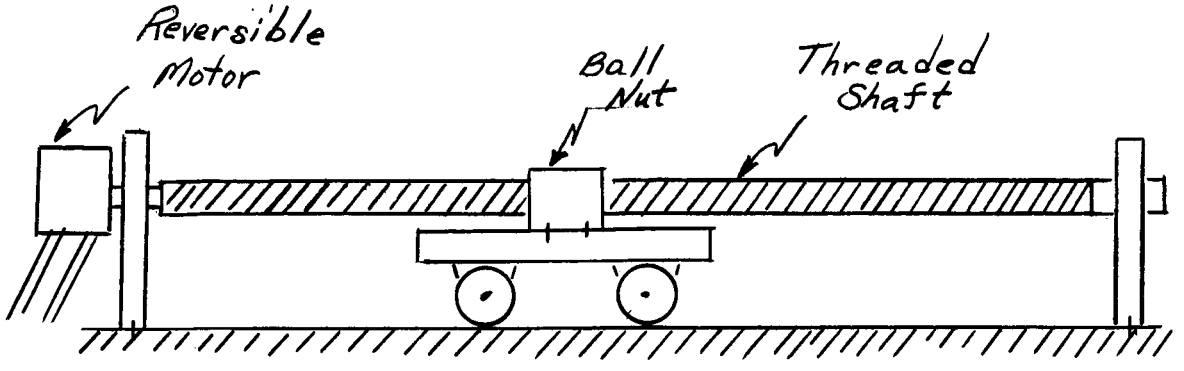

Fig. B-2a. The mechanical features of a threaded shaft and nut drive.

This method of power transmission was studied after a system, similar to that depicted above, was shown to the designers during a tour through the facilities of Grumman Aircraft and Engineering Corporation. Again, simplicity and adaptability to both small and large displacements were the attractive feature of the drive.[7]

The threaded shaft and nut were rejected since 32 foot shafts are not commercially available. The designers also anticipated some difficulty in devising supports for the long threaded member.

B-3 Hydraulic Piston

The family of hydraulic components includes a new type of large displacement hydraulic piston. This device resembles a long sealed tube with a zipper down the side. See Fig. A-3a.

Projecting through the zipper opening is an attachment bar which connects to the load and travels with the piston in the tube.

This system appeared to have all the quick response, high power capabilities characteristic of hydraulic equipment.

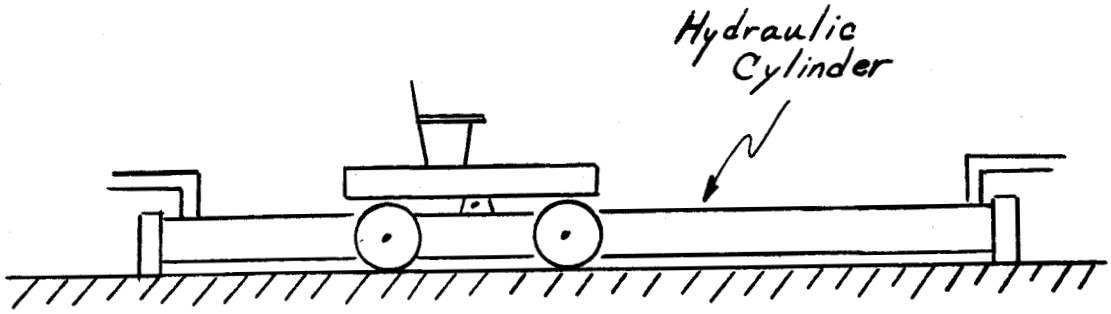

Fig. A-3a. Application of the Hydraulic Piston

Regrettably, the maximum length of tube available was 15 feet. Custom building of a 32 foot piston was beyond the budget of the project.

B-4 Open Wound Induction Motor

The fourth power transmission and supply scheme studied involved application of a solenoid-like device employing alternate current to generate a magnetic field and linear force on a long armature.[8] The reader is referred to the reference for details of the motor's operation. The cart application would have involved a configuration as shown in Fig. A-4a.

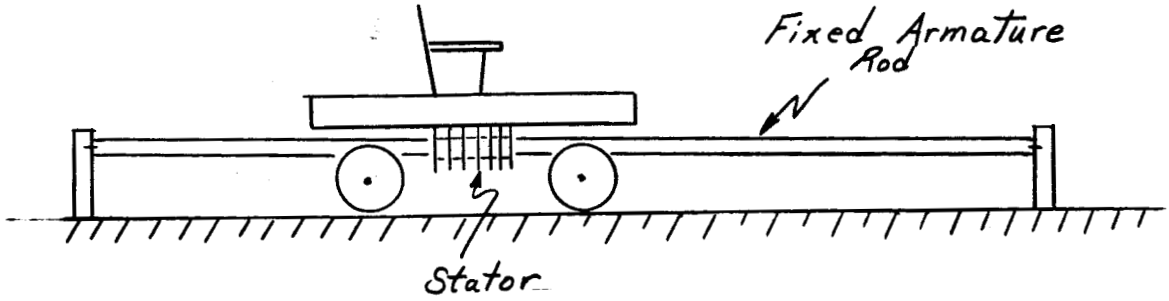

Fig. A-4a. The Open Wound Induction Motor Assembly.

In this case, assembly of short armature rods to a length of 32 feet appeared feasible. The system was attractively simple, combining the power source and transmission equipment in one package. The motor was not used, however, because of the long down times required between strokes to prevent overheating of the stator element.

APPENDIX C

DERIVATION OF THE SPEED AND TORQUE REQUIREMENTS AT THE LOAD DRUM SHAFT

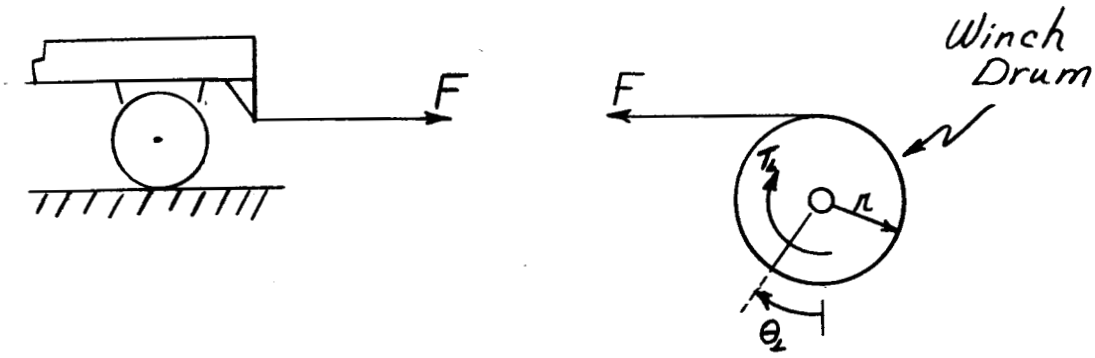

Fig. C-1a. Diagram of the forces and torques at the load drum

The above diagram shows the forces, torques and angular displacements pertaining at the winch or load drum when the cart is undergoing an acceleration. For the purpose of these calculations, the winch drum will be considered to have negligible inertia compared to that of the cart. Stiction and rolling friction will be ignored.

The angular displacement of the winch drum is related to the linear displacement of the cart

$$\theta(t) = \frac{1}{r}\, x(t) \tag{C-1}$$

Differentiating the above expression with respect to time produces the corresponding velocity and acceleration expressions:

$$\dot{\theta}(t) = \frac{1}{r}\, \dot{x}(t) \tag{C-2}$$

$$\ddot{\theta}(t) = \frac{1}{r}\, \ddot{x}(t) \tag{C-3}$$

The accelerating force applied to the cart is just

$$F(t) = m_s \ddot{x}(t) \tag{C-4}$$

This force is generated by a motor acting on the load drum shaft,

$$F(t) = \frac{1}{r} T_L(t) \tag{C-5}$$

where $T_L(t)$ is the torque output of the motor.

Combining equations 4 and 5, the required motor torque can be expressed in terms of the vehicle acceleration

$$T_L = r F(t) = r m_s \ddot{x}(t) \tag{C-6}$$

For $r = 4$ inches, $m_s = 12.4$ slugs, the approximate motor torque and speed requirements can be calculated.

C-1 The Case for Constant Acceleration

$$\ddot{x}(t) = 9.66 \text{ ft/sec}^2 \tag{C-7}$$

$$m_s = 12.4 \text{ slugs}$$

$$(T_L)_{max} = 480 \text{ in. lbs.}$$

$$(\dot{\theta}_L)_{max} = 500 \frac{\text{rev}}{\text{min}}$$

C-2 The Case for Sinusoidal Accelerations

$$\ddot{x}(t) = -X\omega^2 \sin \omega t \qquad (C\text{-}8)$$

$$\ddot{\theta}(t) = -\frac{1}{r} X\omega^2 \sin \omega t$$

$$T_L(t) = -r m_s X \omega^2 \sin \omega t$$

$$\dot{\theta}_L(t) = \frac{1}{r} X \omega \cos \omega t$$

For $\omega = .776$ rad/sec, $X = 16$ ft

$(T_L)_{peak} = 480$ in·lbs

$(\dot{\theta}_L)_{peak} = 360$ rev/min

APPENDIX D

THE DRIVE SYSTEM DESIGN

Along with the detailed specifications, the manned vehicle control laboratory suggested that the cart be conceived and constructed as the load member in a closed loop, position controlled servo. Figure 2.3a shows the location of the drive system in the control circuit and further displays the parallel feedback paths, one all electric and one including the human cart pilot, that close the loop.

From the control block diagram, it is apparent that the collection of elements marked "Drive System" acts as the signal to power transducer. Accepting inputs at signal level from the summing amplifier, the system must deliver, at its output, the torques and speeds demanded at the winch drum shaft.

Two methods of constructing the drive system were studied by the designers. The first method, an all electric configuration, was discarded in favor of one employing high pressure hydraulics, but both methods are discussed here to outline the reasoning behind the design choice.

D-1 The Electric Drive

Initial effort was devoted to the investigation of an electric drive consisting of an amplidyne, a d-c motor and a 4:1 speed reducer. These components were to be arrayed in the drive system as shown in Fig. D-1a.

The reader is referred to the wealth of literature explaining the electro-magnetic principles employed in the amplidyne.[6] The control constants, weights and dimensions of typical

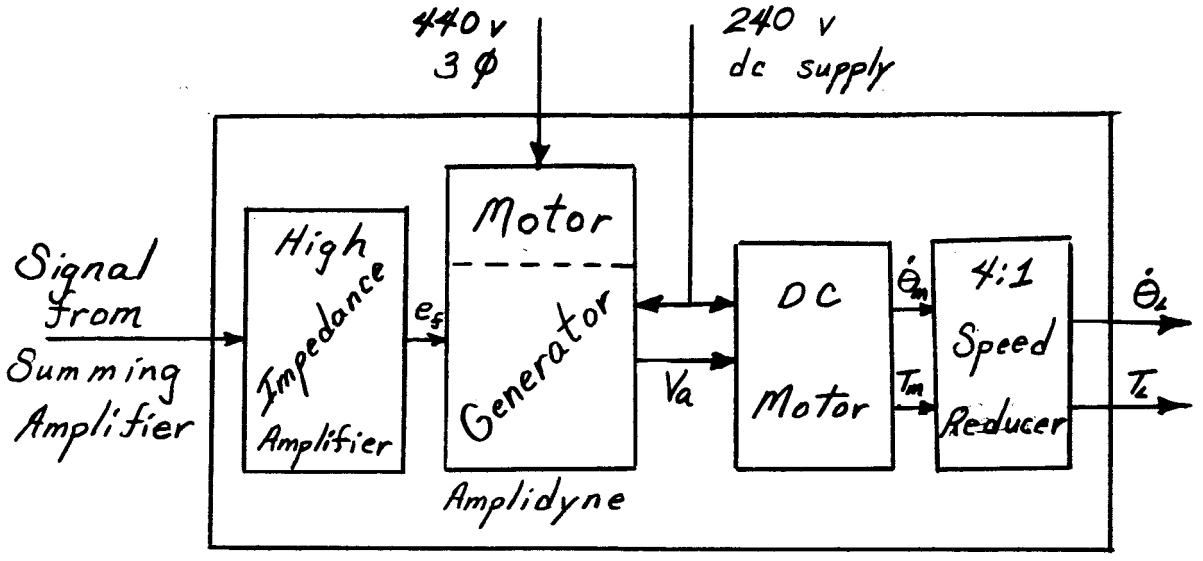

Fig. D-1a. The electric drive system.

amplidynes are available in the General Electric Company's publication "The Amplidyne, Characteristics and Technical Data."

For the purpose of this appendix, the amplidyne can be thought of as a high gain amplifier capable of delivering controlled d-c power over a range of several thousand watts in response to a few milliamps of input current. The amplidyne in this application was postulated as the controller and driver of a separately excited d-c motor—the output voltage of the amplidyne being applied to the armature of the motor.

Cost considerations blocked the purchase of a new amplidyne and motor. Therefore, the design process was inverted and the designers, equipped with the required power ratings, went searching for used equipment prior to any full blown design studies. The search quickly revealed that used equipment in the 4 hp range was not readily available. Machinery at a 2 hp rating was, however, to be found. As 2 hp was sufficient to meet the sinusoidal requirements for the drive, the control design was undertaken using the characteristics of a 2 hp motor and amplidyne. The users accepted the implied constraint on the duration of any constant accelerations to be applied to the vehicle.

Using a linear model for the amplidyne-motor combination, the previously calculated estimates for the load, and the assumption of a high impedance amplifier preceding the amplidyne in the control circuit, a stability study, using root locus techniques, was performed. The open loop performance function and the associated root locus are displayed below.

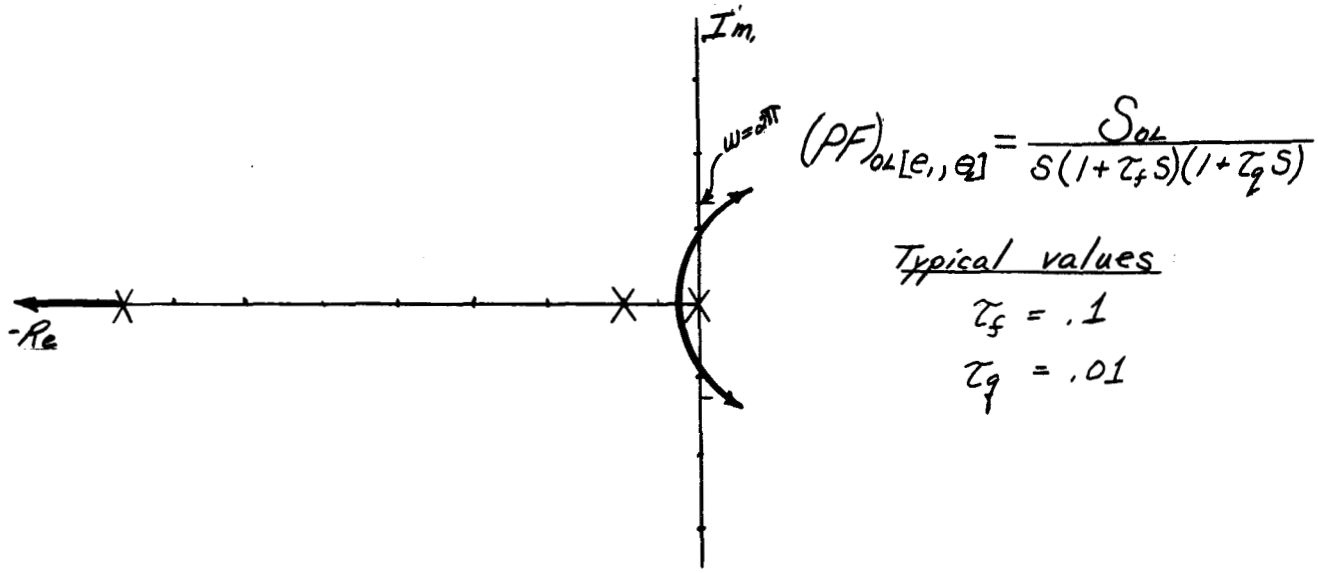

Fig. D-1b. The uncompensated root locus for the amplidyne-motor drive system.

The root locus plot indicated that, uncompensated, the 2 hp amplidyne-motor drive would never meet the frequency specifications laid down by the user. Attempts to achieve stability at one cycle per second by using an amplidyne and motor rated at 4 hp were equally unsuccessful due to the larger inertia introduced with the larger motor.

A second attempt at stabilizing the analytic system via use of a simple pole-zero pair (lead lag network) was more promising. The compensated open loop performance function and the associated root locus appear in Fig. D-1c.

Carried to this point, the design process indicated that the amplidyne motor combination could, with compensation, meet both the sinusoidal power and frequency specifications. The electric system was attractive because the components were compact, clean and readily available. The assembly could be

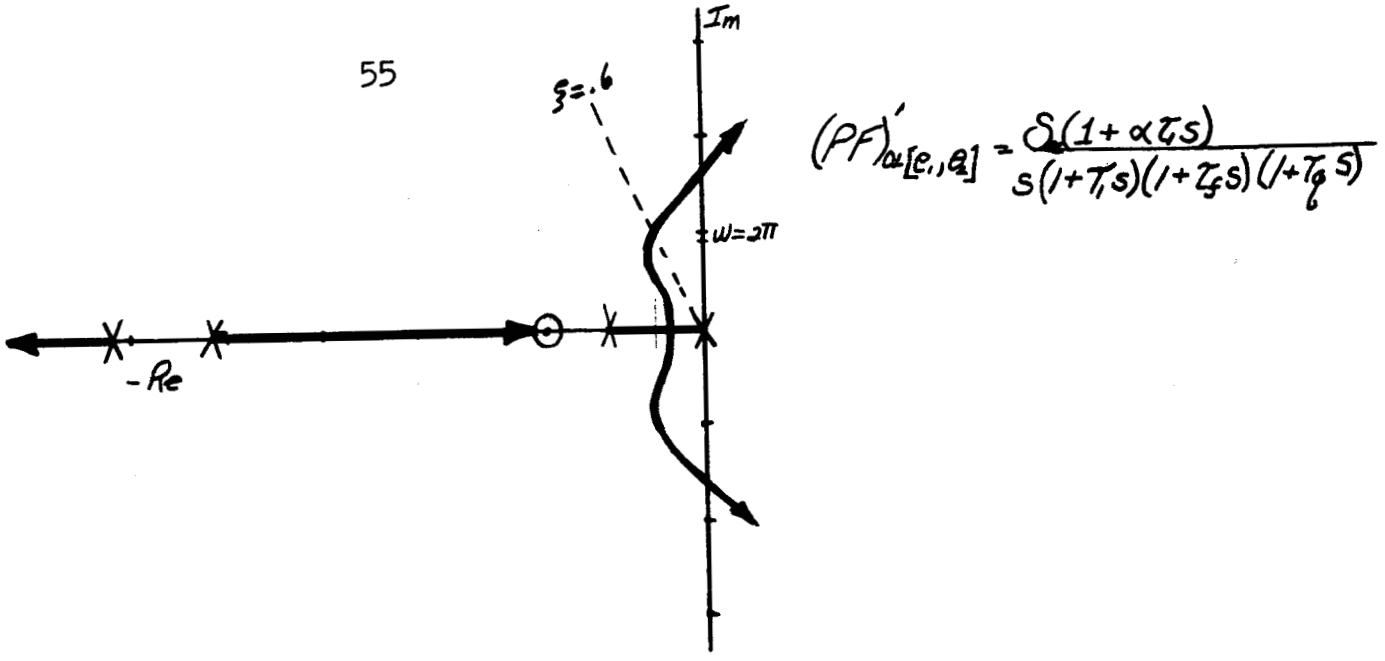

Fig. D-1c. The compensated root locus for the amplidyne-motor drive system.

performed with the advice and help of laboratory personnel familiar with similar equipment.

As noted earlier, however, the available 2 hp machines could not supply the long duration, constant acceleration power requirement of 3.8 hp. In addition, the known load inertia and motor efficiency represented only rough guesses at what the final numbers might be for a completed sled and a used motor. A system rated for only 2 hp was leaving little room for design error and the addition of dead weight.

The drawbacks of the electric system seemed to warrant study of other means for propelling the sled. The hydraulic drive, ultimately assembled, was the product of this study.

D-2 The Hydraulic Drive System

As a substitute for the components shown in the electric drive block diagram, a collection of hydraulic elements was postulated for the hydraulic system. The pertinent block diagram follows.

Again, with cost in mind, the design process started with a search for surplus or used hydraulic equipment. Besides the required valve, motor and speed reducer a source of high pressure

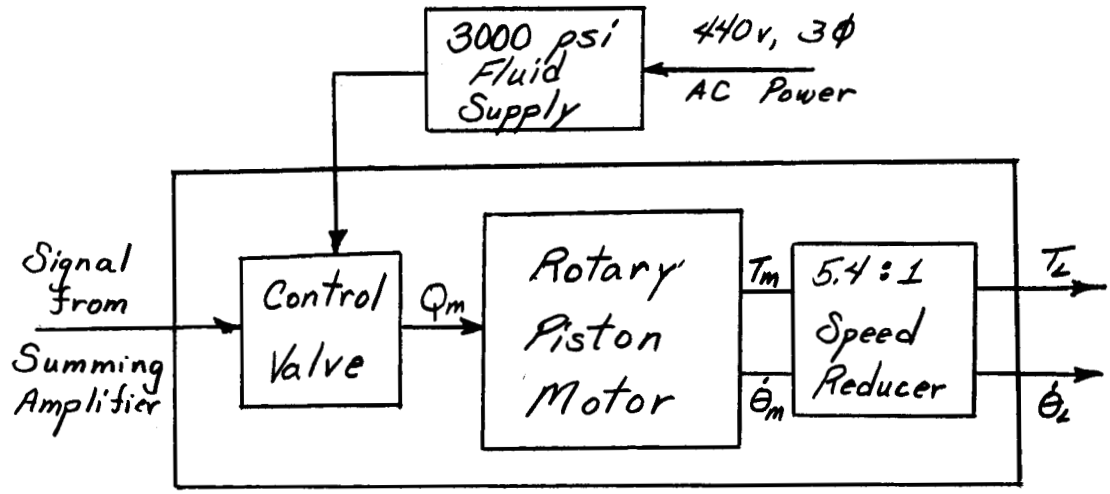

Fig. D-2a. The Hydraulic Drive System.

fluid had to be found. An idle 3000 psi supply pump and rotary piston motor were located. Moved to the laboratory and adapted for the sled system, these two components formed the basis for the final assembly.

The rotary piston motor was of an industrial type for which the frequency characteristics are unknown. From the motor flow and torque ratings, however, the valve flow rate and pressure drop were determined. These values were found for a single operating point as shown in Appendix E. Only this rough estimate of required valve performance was made as the valve secured for the application was also supplied devoid of any pressure-flow characteristics. The designers performed a static, no load test on the valve and used this data with a parabolic approximation to the valve pressure-flow curves to verify that the valve would, at least, handle the one, maximum power load.

The number of unknowns involved in the assembly of the hydraulic system caused the designers to forego a detailed control study. The motor and pump had not been used for an extended period of time. The valve characteristics were not known. The designers proceeded with the assembly hoping to take advantage of the good response, high torque and low inertia characteristics of hydraulic equipment in general. The intelligence in this decision has yet to be proved.

APPENDIX E

DETERMINATION OF THE HYDRAULIC COMPONENT PARAMETERS

E-1 Introduction

The hydraulic system design was a problem in matching given, used equipment to the power, torque and speed requirements calculated in Appendices A and C. The pump, pump drive, and hydraulic motor had previously served as the power source on a precision milling machine. The valve was loaned to the designers for the purpose of testing the system. The speed reducer was purchased from a used machinery dealer. Rough calculations indicated that this collection of equipment would, at minimum, meet the maximum power requirements. These calculations are outlined in the following sections. The designers did not have sufficient information on the components to verify, prior to the testing, that the hydraulic system would meet the sinusoidal specifications.

E-2 The Pump

The hydraulic pump in the circuit diagram of Figure E-3 was supplied on a portable frame complete with a 20 hp electric motor, reservoir and connecting lines. The pump, a product of the Denison Engineering Company, was of the rotary piston type. The manufacturer was unable to identify the pump from the numbers on the case—the nameplate was missing. The previous users, however, indicated that the pump was rated for 3000 psi operation. Proceeding with the pump as a large unknown, the designers replaced the pressure gauge and filter element, and attached new hosing.

E-3 The Hydraulic Motor

The hydraulic motor was also a product of the Denison Engineering Company.

Model: MA-071-340-F (Piston type)
Rated torque: 7.43 inch pounds per 100 psi
Rated flow: .47 in^3 per revolution = d_m
Maximum pressure: 2500 psi
Maximum speed: 3000 rpm = $(\theta_m)_{max}$

In Appendix C, the torque and speed requirements were calculated at the winch drum shaft for the case of maximum power— .3g constant acceleration for 16 feet. The calculations showed that 480 inch pounds at 500 rpm would meet the load condition.

Examination of the motor nameplate data immediately suggested the use of a speed reducer in the ratio of 5 or 6 to 1 between the motor and the winch drum shaft. To allow for design errors, additional loading of the sled, loss of motor efficiency at low speeds and torque losses in the speed reducer, the designers had decided to overbuild the system by a factor of 1.5. A speed reducer in the ratio of 5:1 would permit the system to deliver up to 37.15 inch pounds per 100 psi at the load drum of the winch. With 2000 psi pressure drop across the motor, the system would have a torque capability of 740 inch pounds—near enough to the "overbuild" requirement of 1.5 x 480 = 660 inch pounds.

E-4 The Speed Reducer

The designers located a used herringbone speed reducer. The reducer had a reduction ratio of 5.4:1 rather than 5:1. The former ratio was accepted, however, as the reducer was in good condition and available at low cost.

E-5 The Hydraulic Valve

With the motor and speed reducer selected, the design task was reduced to finding a suitable control valve. At the maximum winch speed of 500 rpm, the motor would be turning at 2700 rpm. The flow rate through the motor at this speed is the product of the motor flow per revolution and the angular speed

$$d_m \times \theta_m = .47 \text{ in}^3/\text{rev} \times 2700 \text{ rev/min} \qquad (E.1)$$
$$= 1270 \text{ in}^3/\text{min} \quad \text{or} \quad 21.2 \text{ in}^3/\text{sec}$$

To sustain the case of constant acceleration at .3g's, a pressure drop of 2000 psi across the motor is required. (Remember this includes the 1.5 "overbuild" factor.) For a system pressure of 3000 psi, the valve drop is restrained to be no greater than 1000 psi. (A good rule of thumb is to expect that 1/3 of the pressure drop occurring between the pump and the reservoir takes place across the valve—assuming negligible line losses.)

Figure E-5a displays the family of flow-pressure curves for a typical four way spool valve.

The curves can be expressed mathematically by

$$Q_m^2 = P_s - C(z) P_m \qquad (E.2)$$

where

P_s = supply pressure in psi
P_m = pressure drop across the motor in psi
Q_m = flow rate through the motor and valve in in^3/sec
$K(z)$ = proportionality factor dependent, among other things, on the linear displacement, z, of the valve spool from its closed position.

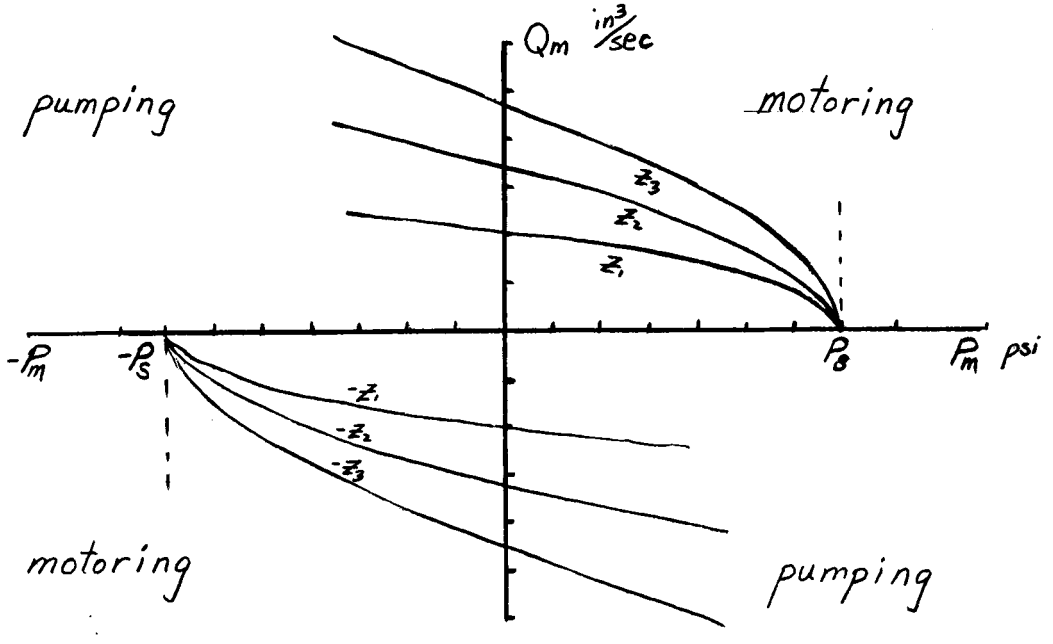

Figure E-5a. The flow-pressure curves for a four way spool valve operating from a constant pressure supply.

The valve sought by the designers, following the flow and pressure calculations, had to be capable of delivering 21.2 in^3/sec at a load pressure drop of 2000 psi. This operating point had to lie within the envelope of flow-pressure curves for the valve finally selected.

A Moog valve (Model 2004A) was available to the designers without cost. The above operating point was found to lie within the envelope of curves for this valve as shown in Figure E-5b. The valve was rated for only 2700 psi.

The Moog valve was employed during early testing of the control system. A failure in the valve flapper required that the device be returned to the manufacturer for repair. The tests were completed with a second valve which had a restrictive flow rate.

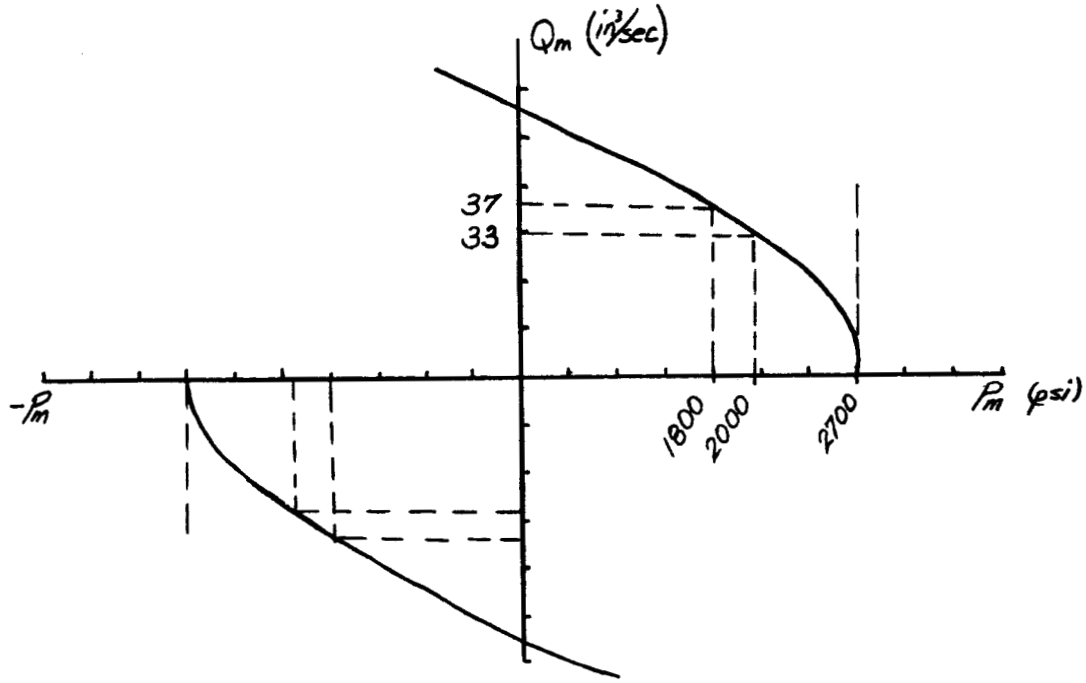

Figure E-5b. The theoretical maximum flow rate curve for Moog valve Model 2004A.

E-6 Operating Instructions

The hydraulic circuit diagram of Figure E-6a is annotated with the letters A through H which are also clearly marked on the assembled control system. The letters mark valves and switches to be operated in starting the hydraulic controls. These letters are also mentioned in the operating instructions below.

In starting:

(a) Clear the track area of obstructions and post the No Smoking sign prior to starting the pump.

(b) Verify that the Roll Simulator power switch is in the OFF position.

(c) Close the main switch marked A on the 440 volt power bank.

(d) Completely open the hand valves labelled B and C at the pump station. Open the hand valves marked D, E and F at the valve manifold.

(e) Verify that the valve electrical control switch marked G is in the OFF position.
(f) Start the pump by depressing the brown button on the motor starter marked H.
(g) Using valve B, increase the line pressure to 500 psi. Check all fittings for leaks.
(h) If the hydraulic motor is turning slowly, center the valve using the mechanical adjustment at the rear of the manifold. The motor rotation should stop.
(i) By slowly closing valve B, raise the line pressure to the desired operating level as displayed on the pressure gauge. Again check for leaks.
(j) Close switch G and proceed with the test.

To stop the system:

(a) Return switch G to the OFF position.
(b) Open valve B and reduce the line pressure to zero.
(c) Stop the pump by depressing the red button on the motor control marked H.
(d) Return switch A to the OFF position.

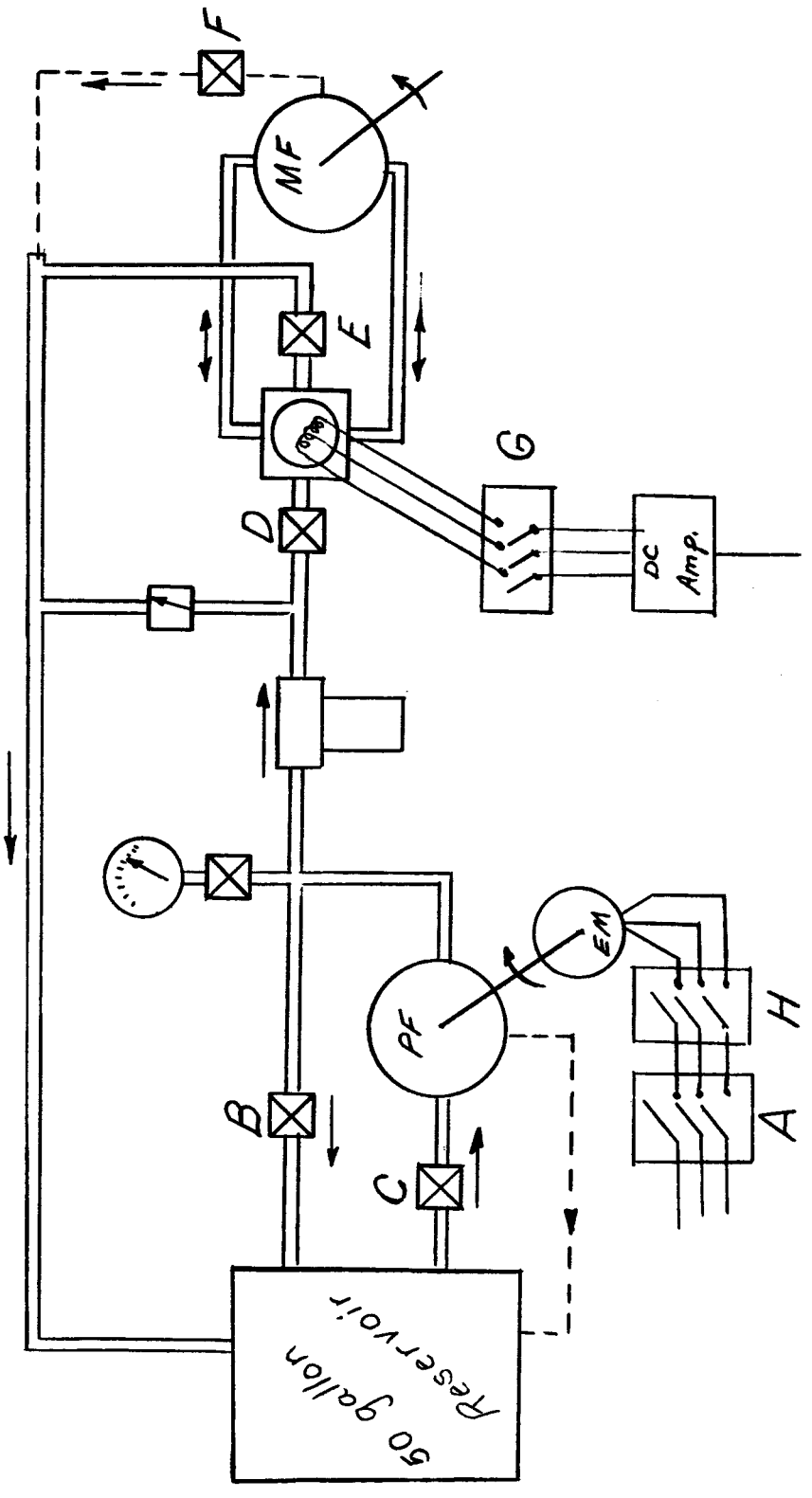

Figure E-6a. The hydraulic circuit diagram

APPENDIX F

VIBRATION CONTROL CALCULATIONS

(1) General

Assume sinusoidal wave form $X = A \sin \omega t$ (F·1)

$$\therefore \quad \dot{X} = A\omega \cos \omega t$$

$$\ddot{X} = -A\omega^2 \sin \omega t \quad \text{(F·2)}$$

peak displacement $= A$

and peak acceleration $= \ddot{X}_{MAX} = A\omega^2$ (F·3)

Threshold level $= 10\ cm/sec^2$ OR $\cdot 01g$

Then: $$A = \frac{\ddot{X}_{MAX}}{\omega^2} = \frac{\cdot 01g}{\omega^2}$$

$$\cdot 01g = \cdot 322\ Ft/sec^2$$

$$\therefore \quad A = \frac{\cdot 322}{\omega^2} \quad \text{(F·4)}$$

TABLE OF MAX ALLOWABLE DISPLACEMENTS

FOR .01g ACCELERATION

Acc.	f(cps)	ω	ω^2	A(ft)	A(in)	f(cpm)
.01g	.01	.02π	.00394	81.6	980	.6
.01g	.1	.2π	.394	.816	9.8	6
.01g	.5	π	9.85	.0317	.381	30
.01g	1	2π	39.4	.00816	.098	60
.01g	3	6π	355	.000907	.0108	180
.01g	5	10π	985	.000328	.00394	300
.01g	10	20π	3940	.0000816	.00098	600
.01g	20	40π	15,800	.0000204	.000245	1200
.01g	40	80π	63,000	.00000511	.0000613	2400
.01g	50	100π	98,500	.00000328	.0000393	3000
.01g	60	120π	142,000	.00000226	.0000272	3600
.01g	.9	1.8π	32	.01	.12	54
.01g	.8	1.6π	25.2	.0128	.153	48
.01g	.7	1.4π	19.3	.0167	.20	42
.01g	.6	1.2π	14.2	.0227	.272	36
.01g	.5	---	---	---	---	---
.01g	.4	.8π	6.3	.0511	.614	24
.01g	.3	.6π	3.54	.091	1.09	18
.01g	.2	.4π	1.575	.204	2.45	12

From the data in this table graphs No. F-1 and F-2 were plotted.

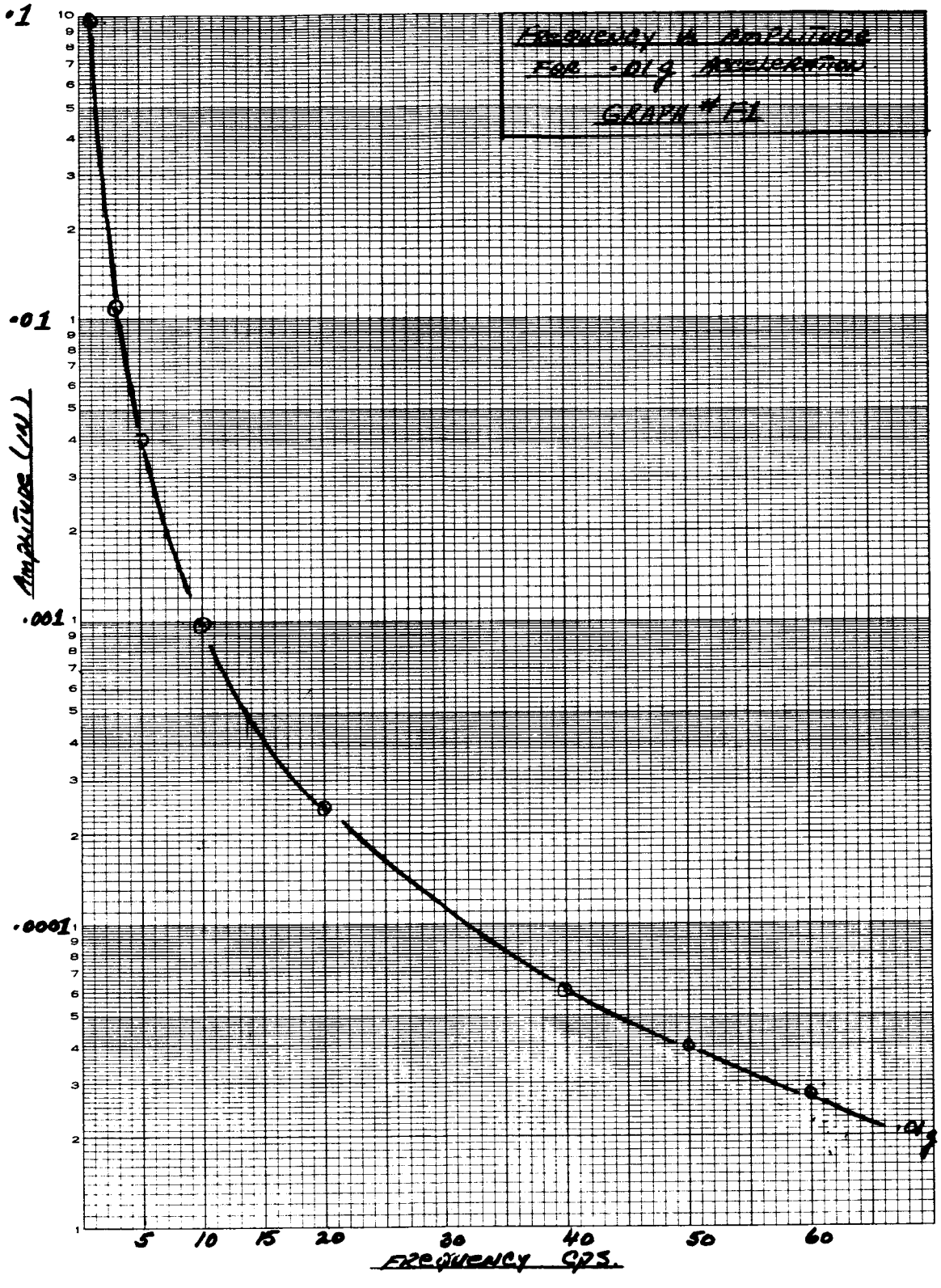
Frequency vs Amplitude
for .01 g Acceleration
GRAPH # 51
.1
.01
.001
.0001
Amplitude (in)
5
10
15
20
30
40
50
60
Frequency CPS.
.01 g

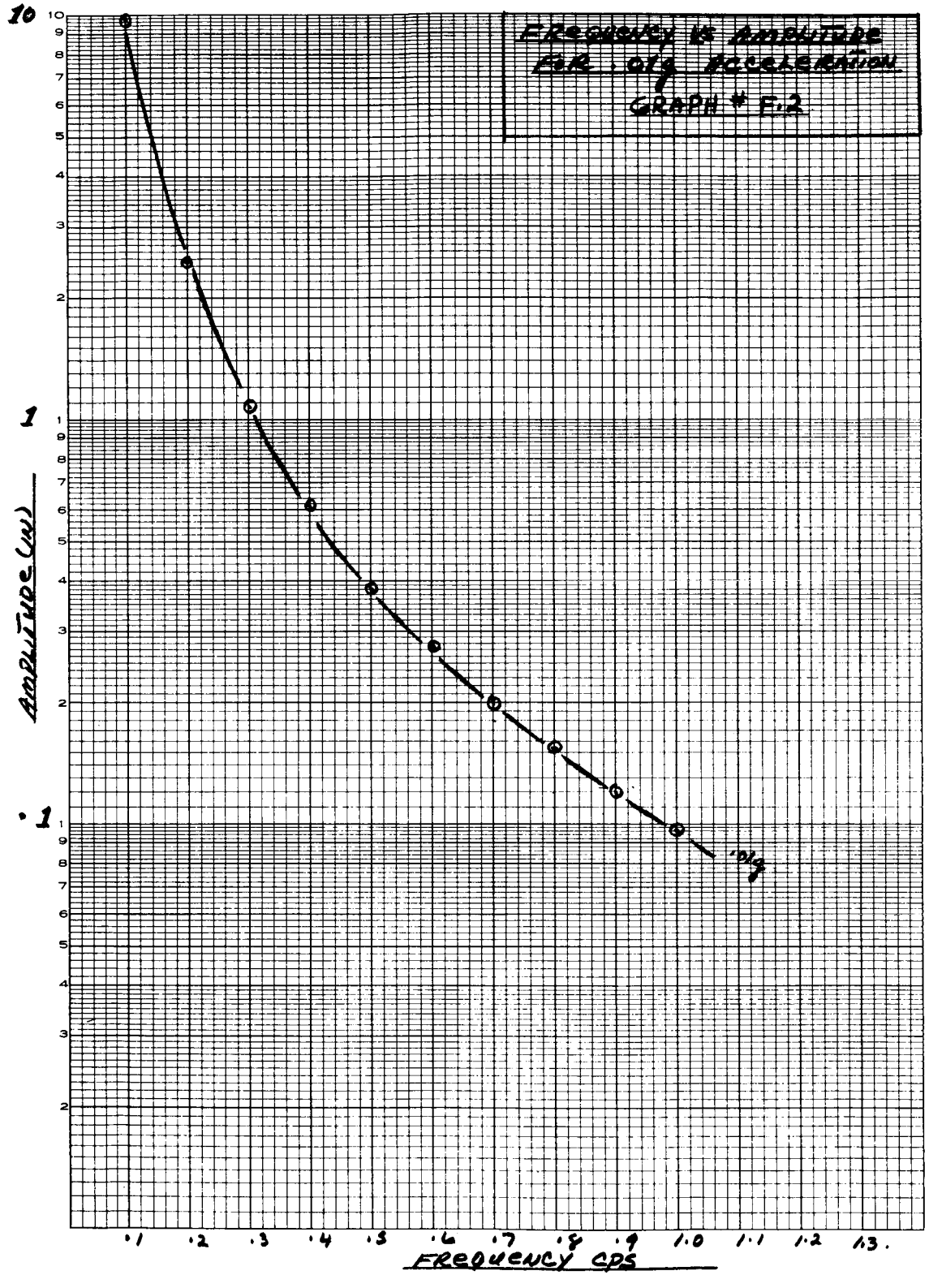
FREQUENCY VS AMPLITUDE
FOR .01g ACCELERATION
GRAPH # F.2
10
1
.1
AMPLITUDE (in)
.01g
.1 .2 .3 .4 .5 .6 .7 .8 .9 1.0 1.1 1.2 1.3.
FREQUENCY CPS

(2) Eccentricity Calculations

Assume wheel RADIUS (r) = 8 IN

Peak velocity $\cong$ 16 f.p.s.

$$V_{MAX} = r\,\omega_{MAX} \qquad \text{(F.5)}$$

OR $\quad 16 = \frac{2}{3}\omega_{MAX}$

$\therefore\ \omega_{MAX} \cong 24$ RAD/SEC

OR $\quad f_{MAX} = \frac{24}{2\pi} = 3.82$ C.P.S.

Using this type of calculation, the following table was obtained for various wheel diameters.

Maximum frequencies for various diameter wheels

Wheel diameter	f_{max}
16"	4 cps
12"	5.5 cps
8"	8.0 cps

Using these characteristic frequencies and referring to graph which gives the allowable disturbances for .01g acceleration, the following table was obtained, assuming a single "lump" or disturbance on the wheel surface.

Maximum disturbance amplitude toleration for various diameter wheels for .01g acceleration

Wheel diameter	Max amplitude of disturbance
16"	.006"
12"	.0035"
8"	.00155"

APPENDIX G

STRUCTURAL CALCULATIONS

Maximum deflection under load [3]

1. Main structural members

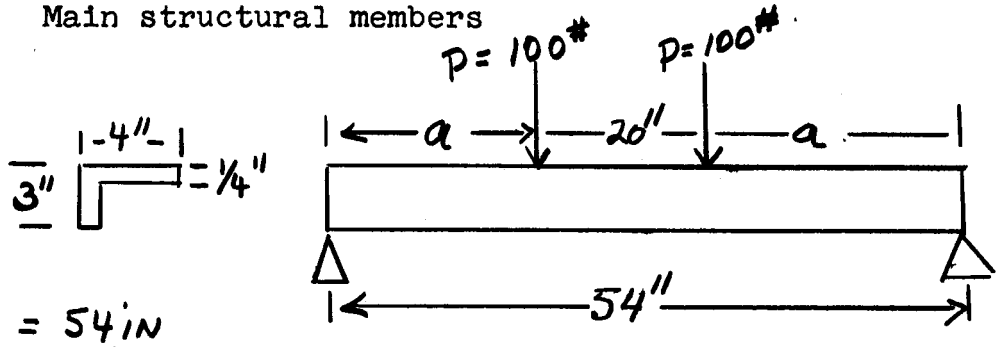

$L = 54$ IN

$a = 17$ IN

$E = 10.4 \times 10^6$ #/IN^2 (FOR 17ST ALUMINUM)

$I = 1.29$ IN^4

$$D_{MAX} = \frac{P}{24EI}(3L^2 - 4a^2) \qquad (G.1)$$

$$\therefore D_{MAX} = \frac{100(17)}{24(10.4)10^6 1.29}\left[3(54)^2 - 4(17)^2\right]$$

$$= 5.28 \times 7600 \times 10^{-6}$$

$$D_{MAX} = .040 \text{ IN}$$

$$\text{NATURAL FREQUENCY } (f_N) \cong \frac{3.13}{\sqrt{D}} \qquad (G.2)$$

$$\therefore f_N = \frac{3.13}{\sqrt{.040}} = 15.7 \text{ cps}$$

USING 61ST ALUMINUM WITH $E = 10 \times 10^6$ THE

MAXIMUM DEFLECTION AND NATURAL FREQUENCY BECOME:

$$D_{MAX} = .0415 \text{ IN}$$

$$f_N = 15.3 \text{ C.P.S.}$$

2. Cross members.

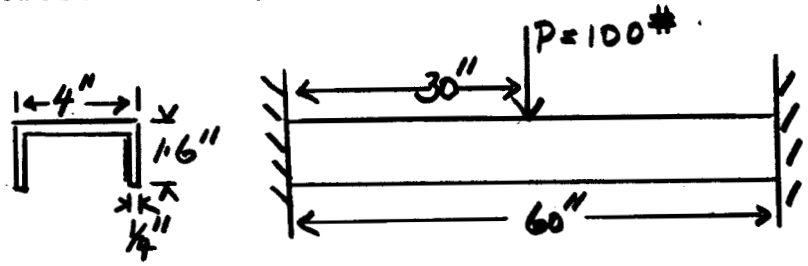

$L = 60 \text{ IN}$

$E = 10.4 \times 10^6$ (FOR 17ST ALUMINUM).

$I = 0.37 \text{ IN}^4$

$$D_{MAX} = \frac{PL^3}{192EI} \qquad (G.3)$$

$$\therefore \quad D_{MAX} = \frac{100(60)^3}{192(10.4)10^6(.37)} = \frac{21.6}{192(10.4)(.37)}$$

$$= .0292$$

$$\therefore \quad D_{MAX} = .0292 \text{ IN}$$

$$\text{NATURAL FREQUENCY } (f_N) \cong \frac{3.13}{\sqrt{D}}$$

$$\therefore \quad f_N \cong 18.2 \text{ CPS}$$

USING 61ST ALUMINUM WITH $E = 10 \times 10^6$ THE MAXIMUM DEFLECTION AND NATURAL FREQUENCY BECOME:

$$D_{MAX} = .0304 \text{ IN} \quad \& \quad f_N = 18 \text{ C.P.S.}$$

Carriage Weight

20' - 4 x 3 x 1/4 61 st aluminum angle at 2.05 lb/ft		41.0 pounds
10' - 4 x 1.6 x 1/4 61st aluminum "U" channel at 2.22 lb/ft		22.2
4 ea Lauco balloon wheels and caster assy's at 7.5 lbs ea		30.0
1 ea 24" x 24" x 1/4" 61st aluminum plate at 3.65 lb/ft^2		14.2
	TOTAL	107.4 pounds

APPENDIX H

Safety Device Calculations

$$V_{MAX} = \dot{x}_{MAX} = 16 \text{ f.p.s} \qquad (H\text{-}1)$$

$$V = at$$

$$a = V/t$$

$$S = \text{DISTANCE} = \tfrac{1}{2}at^2 = \tfrac{1}{2}vt \qquad (H\text{-}2)$$

$$\text{STOPPING DISTANCE} = 4 \text{ ft.}$$

$$\therefore \quad 4 = \tfrac{1}{2}16\,t$$

$$\text{OR} \quad t = 4/8 = \tfrac{1}{2} \text{ sec.}$$

$$\therefore \quad a = \frac{V}{t} = \frac{16}{1/2} = 32 \text{ ft/sec}^2$$

Using this type of calculation we get

stopping distance	acceleration ft/sec^2	~g's
4 ft	32	1
2 ft	64	2
1 1/2 ft	85.4	2.65
1 ft	128	4

After installing the equipment it was found that the vehicle had to be stopped within 1 foot. Thus:

Max wt. = 400 lb
Max mass = $400/g$

$\therefore$ Maximum stopping force required $F_{max} = ma_{MAX}$

$$F_{max} = \frac{400}{g} \times 4g = 1600 \text{ lbs}$$

From load-elongation chart for shock absorber cord.
For 100 per cent elongation
1/2" cord - 240 lb
5/8" cord - 328 lb

$\therefore$ In order to obtain at least 1600 lb stopping force, we must use

4 ea 5/8" cord - 1310 lbs
2 ea 1/2" cord - 480
1790 lbs

This gives 1790/400 = 4.5 g's deceleration.

Chart A-308-4

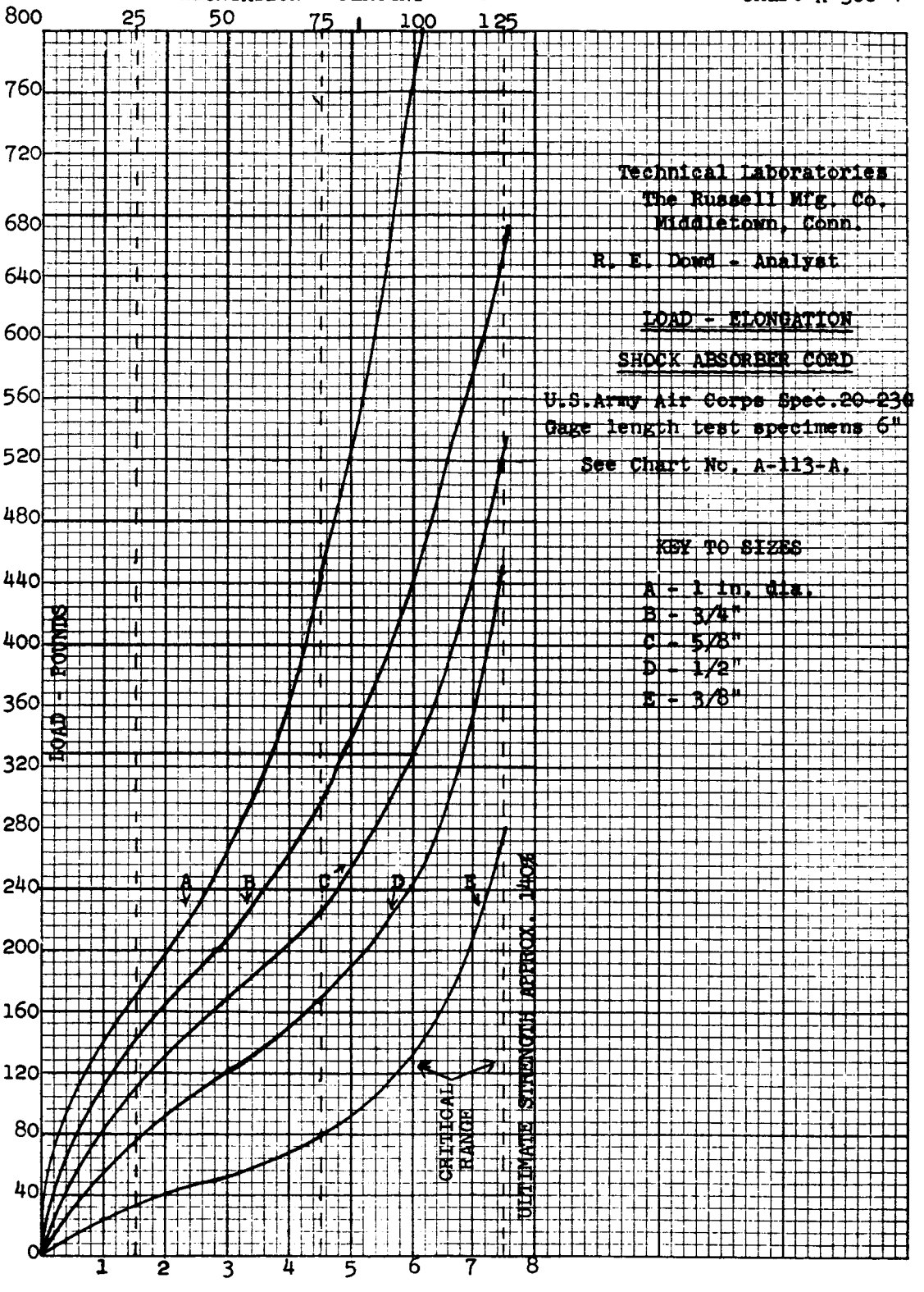
ELONGATION - PERCENT
25
50
75
100
125
800
760
720
680
640
600
560
520
480
440
400
360
320
280
240
200
160
120
80
40
0
LOAD - POUNDS
1
2
3
4
5
6
7
8
A
B
C
D
E
CRITICAL RANGE
ULTIMATE STRENGTH APPROX. 1400#
Technical Laboratories
The Russell Mfg. Co.
Middletown, Conn.
R. E. Dowd - Analyst
LOAD - ELONGATION
SHOCK ABSORBER CORD
U.S.Army Air Corps Spec.20-230
Gage length test specimens 6"
See Chart No. A-113-A.
KEY TO SIZES
A - 1 in. dia.
B - 3/4"
C - 5/8"
D - 1/2"
E - 3/8"

APPENDIX I

Test Data

I-1 Introduction

The open loop frequency response tests described in Chapter 4 generated a set of oscillograph tapes. (The low flow rate valve was used.) These tapes displayed, concurrently, the waveform of the valve input signal and the vehicle position for the test frequencies of .33, .5, 2, and 3 cycles per second. The corresponding peak to peak position and power amplitudes appear in Fig. I-2a. Samples of these tapes appear in Figures I-1a and I-1b.

The tests were conducted at a constant pressure of 1500 psi.

Other parameters were:

Position potentiometer excitation:	12 volts
Rated valve current:	5 milliamps
Valve resistance:	1500 ohms.

I-2 Calculations

The oscillograph tapes were examined to determine amplitude and phase information. A Bode plot of the amplitude and phase information versus frequency was produced using the definitions:

(i) $20 \log_{10}(AR) = 20 \log_{10}\left[\frac{\text{Vehicle position amplitude, (feet)}}{\text{Valve input signal amplitude (volts)}}\right]$

(ii) ϕ = phase angle by which the output position lags the input voltage in degrees.

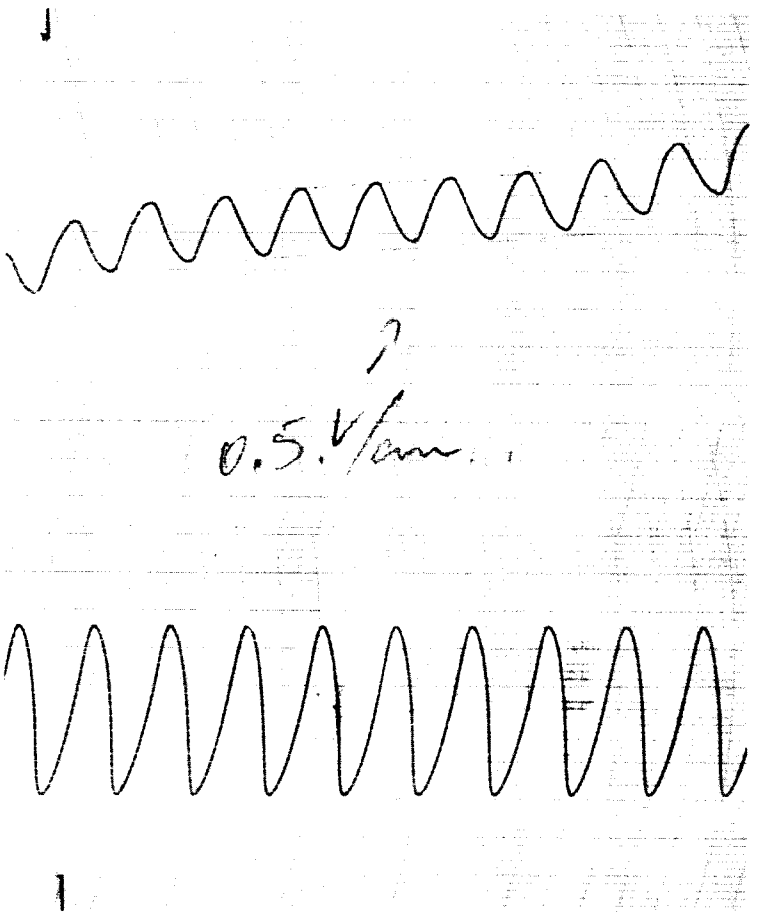

Figure I-1a. Response of the loaded cart at .5 cps. Upper channel gives the cart position, Lower channel displays the valve input voltage vs. time.

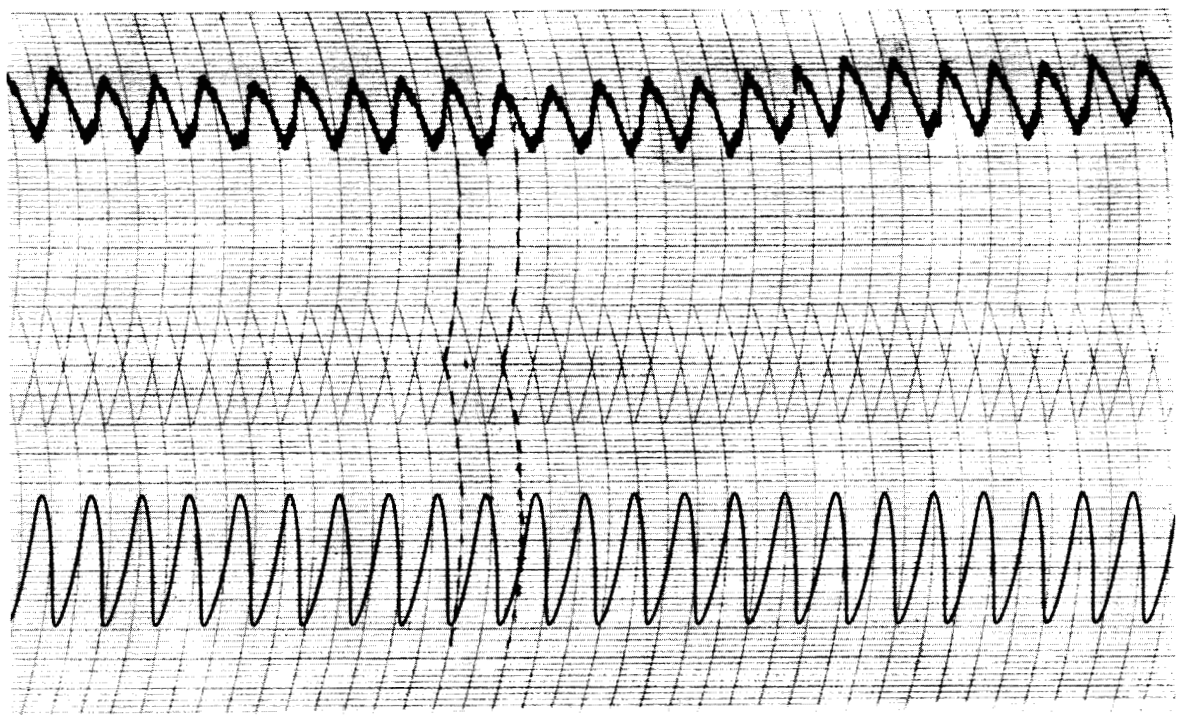

Figure I-1b. Response of the loaded cart at 3 cps. Upper channel gives the cart position. Lower channel displays the valve input voltage versus time.

The tape data is summarized in Figure I-2a. The Bode plot appears as Graph I-1.

Frequency (cps)	Peak Power (hp)	Vehicle Position Amplitude [peak to peak] (ft)	Valve Signal Amplitude [peak to peak] volts	$20 \log_{10}(AR)$	Φ [lagging] (deg)
.33	.105	2.36	4.5	-5.6	90
0.5	.092	1.18	4.5	-11.6	90
1.0	.029	.24	4.5	-25.5	120
2.0	.020	.07	4.5	-36.2	150
3.0	.004	.03	4.5	-44.4	160

Figure I-2a. Data summary for the open loop frequency response tests.

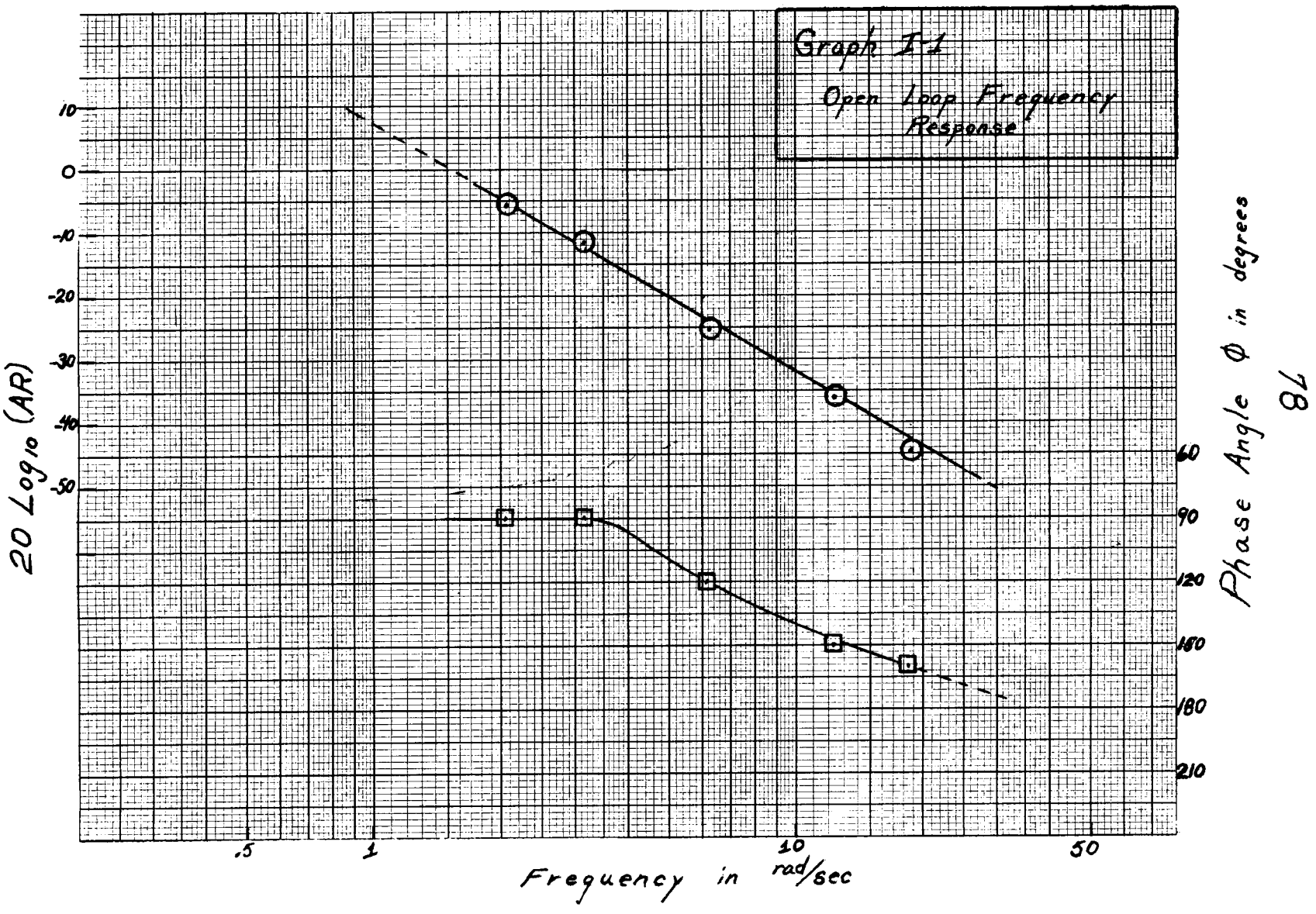
Graph I-1
Open Loop Frequency Response
10
0
-10
-20
-30
-40
-50
20 Log10 (AR)
60
90
120
150
180
210
Phase Angle Φ in degrees
.5
1
10
50
Frequency in rad/sec

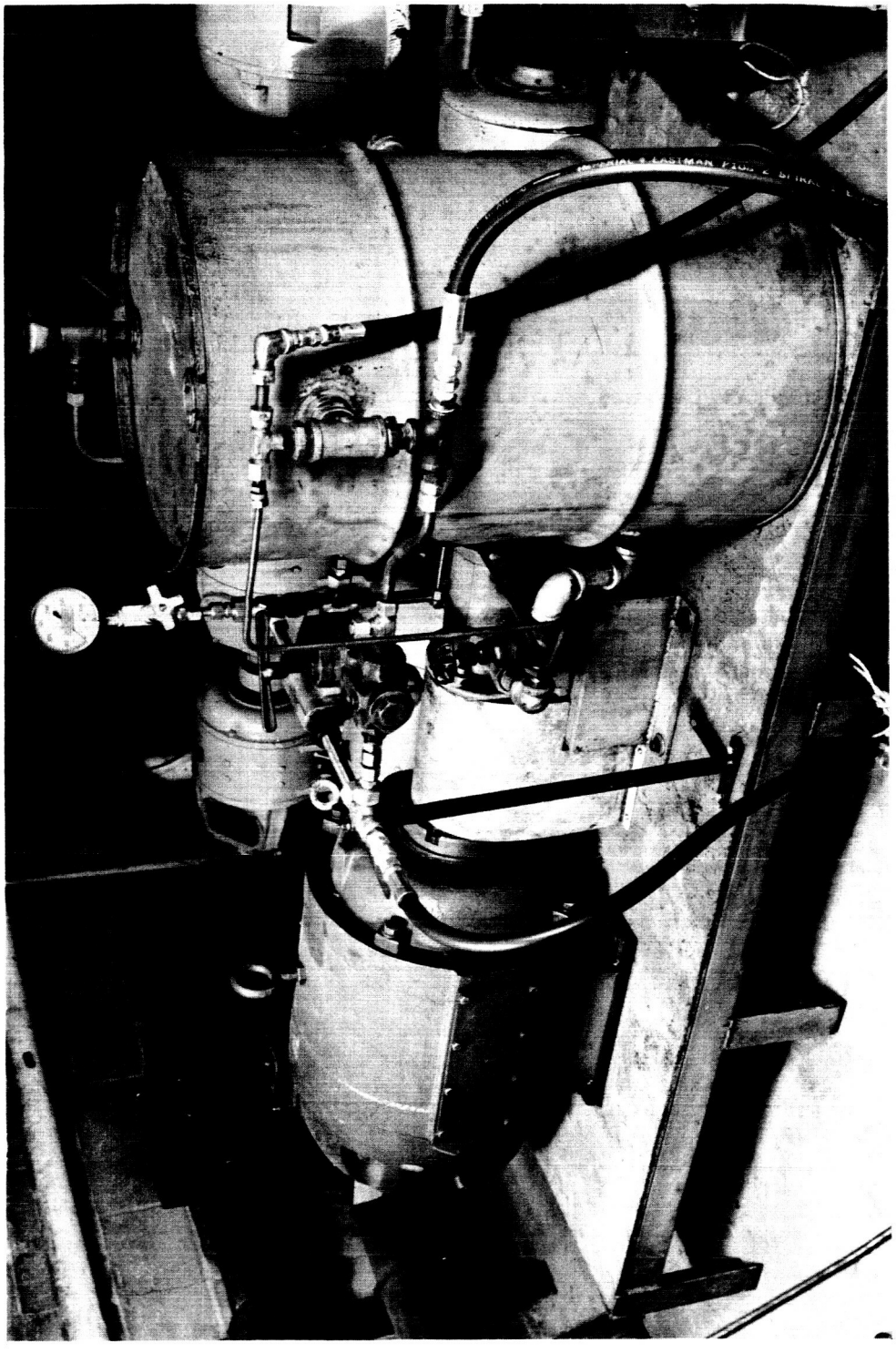

FIG. 1 PUMP ASSEMBLY

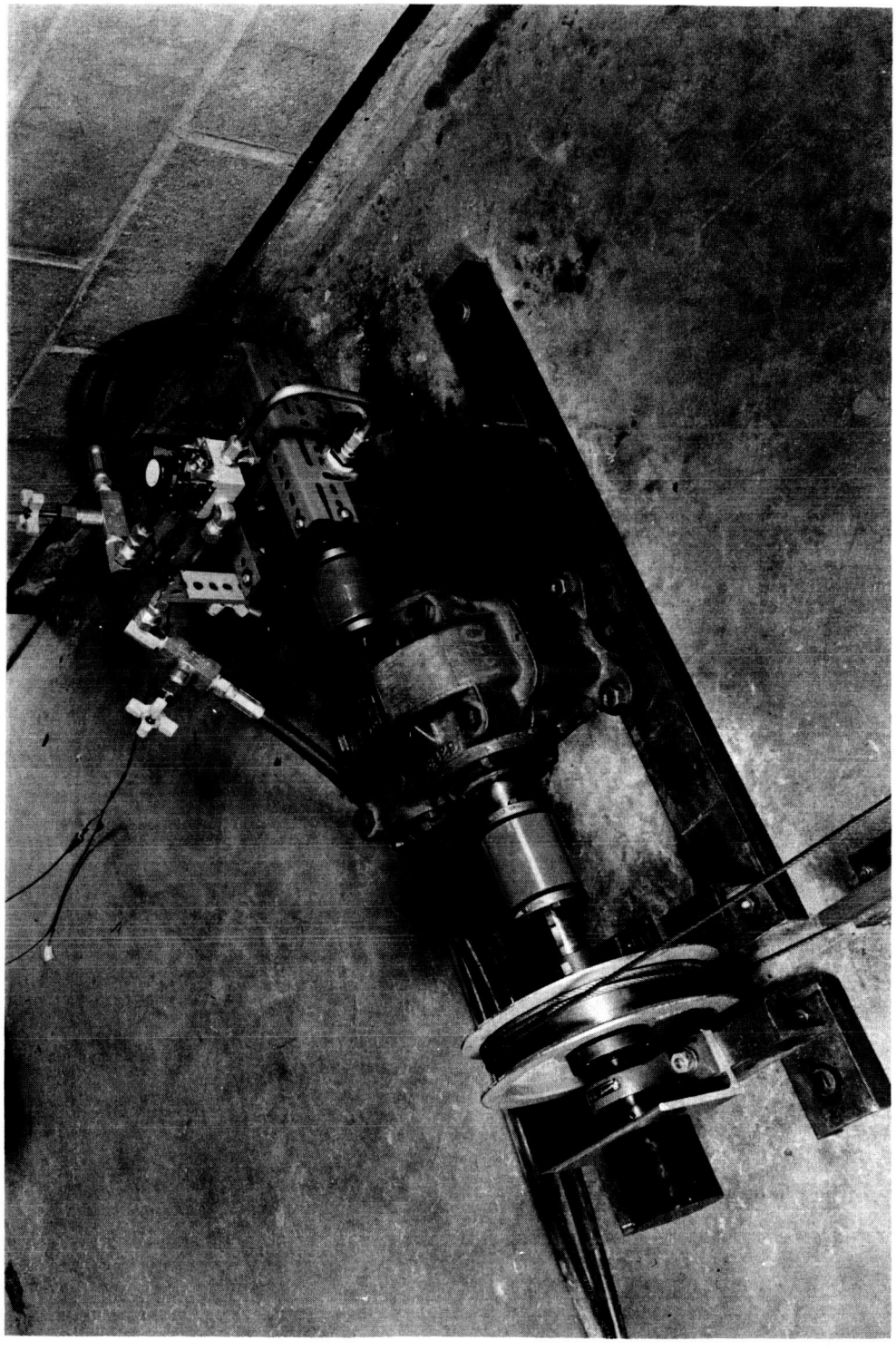

FIG 2 MOTOR & DRIVE ASSEMBLY

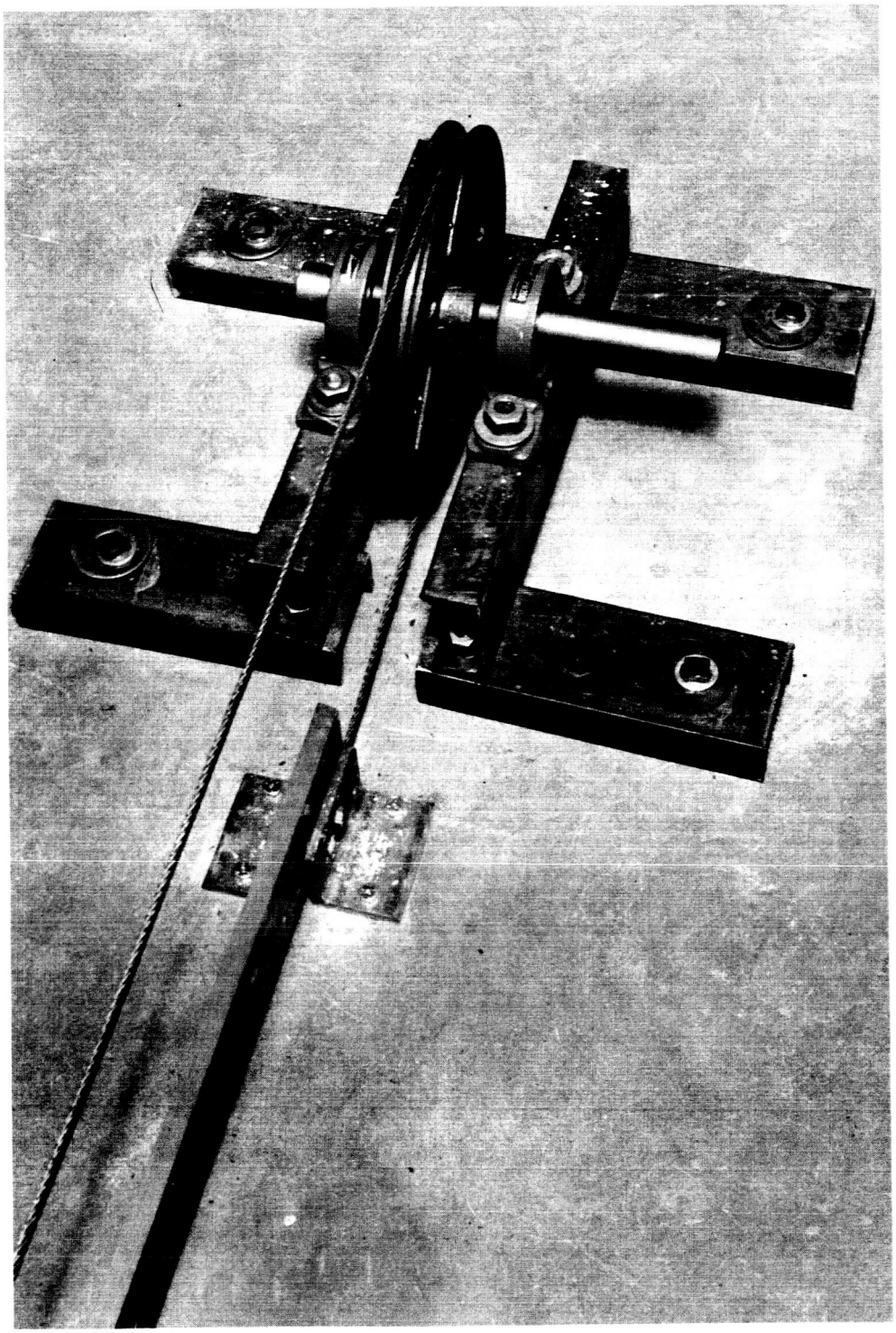

Fig 3 Dummy Pulley

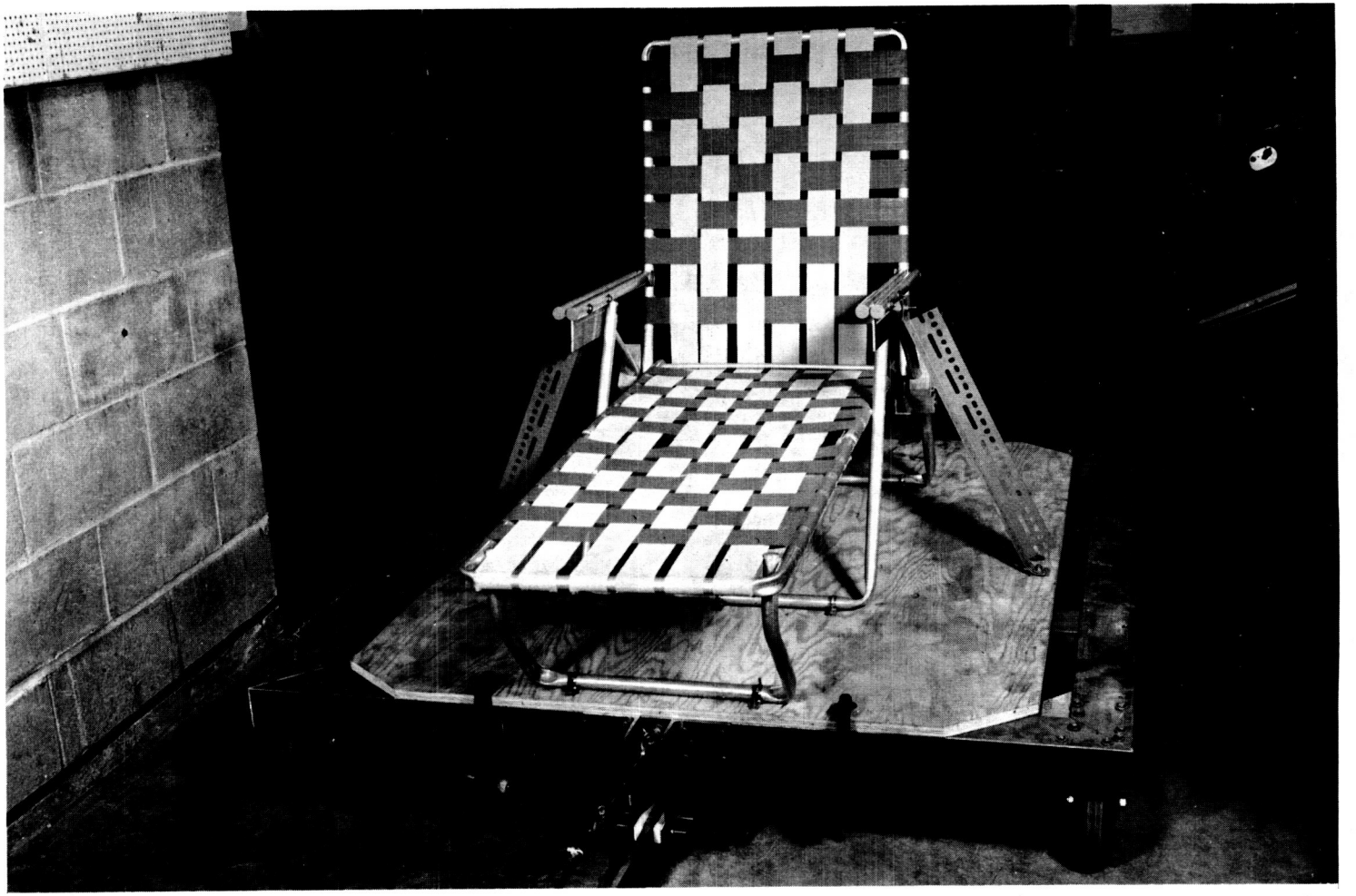

Fig 4 Assembled Vehicle

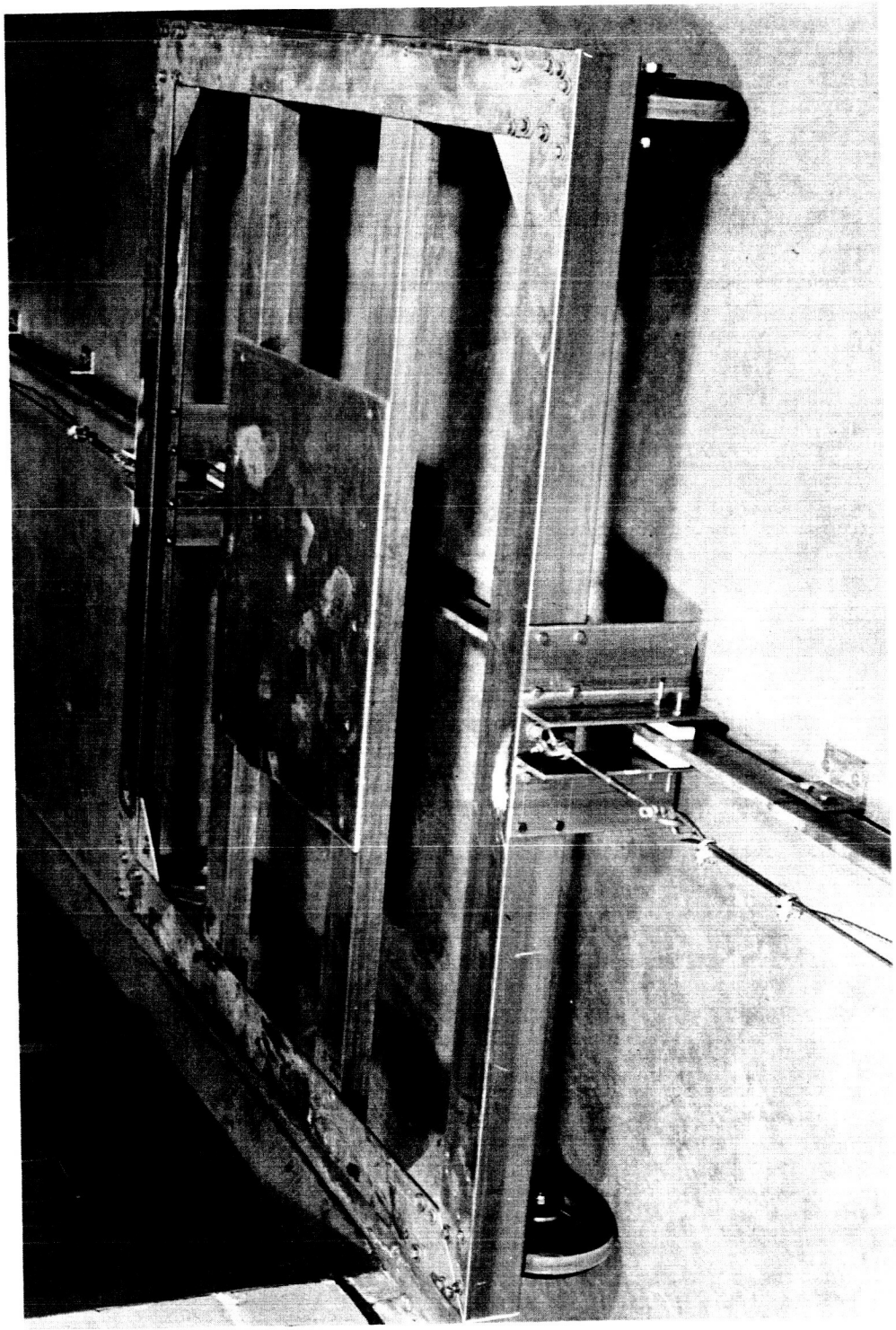

Fig. 5 Vehicle Carriage

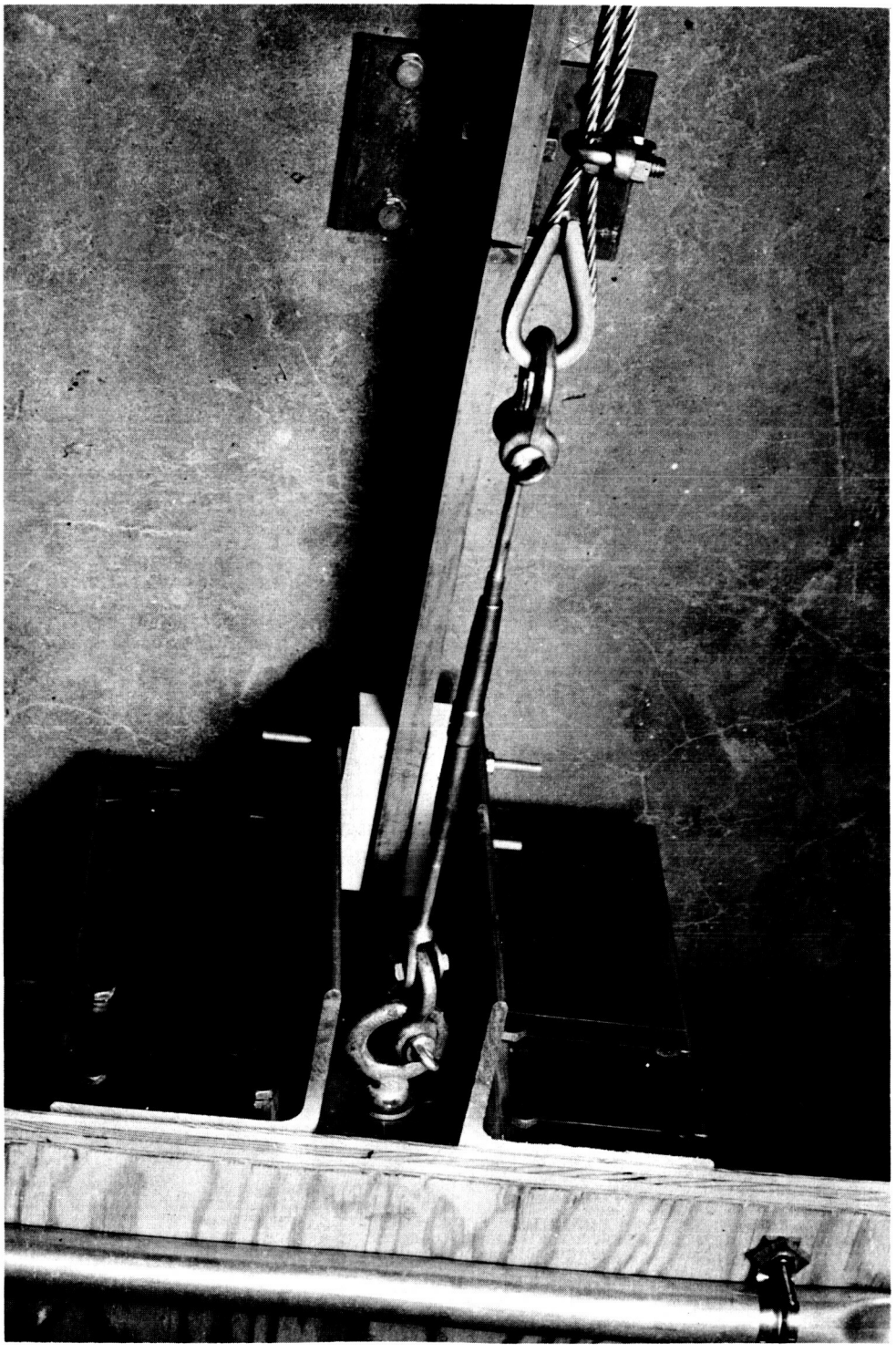

Fig 6 Guide Vanes

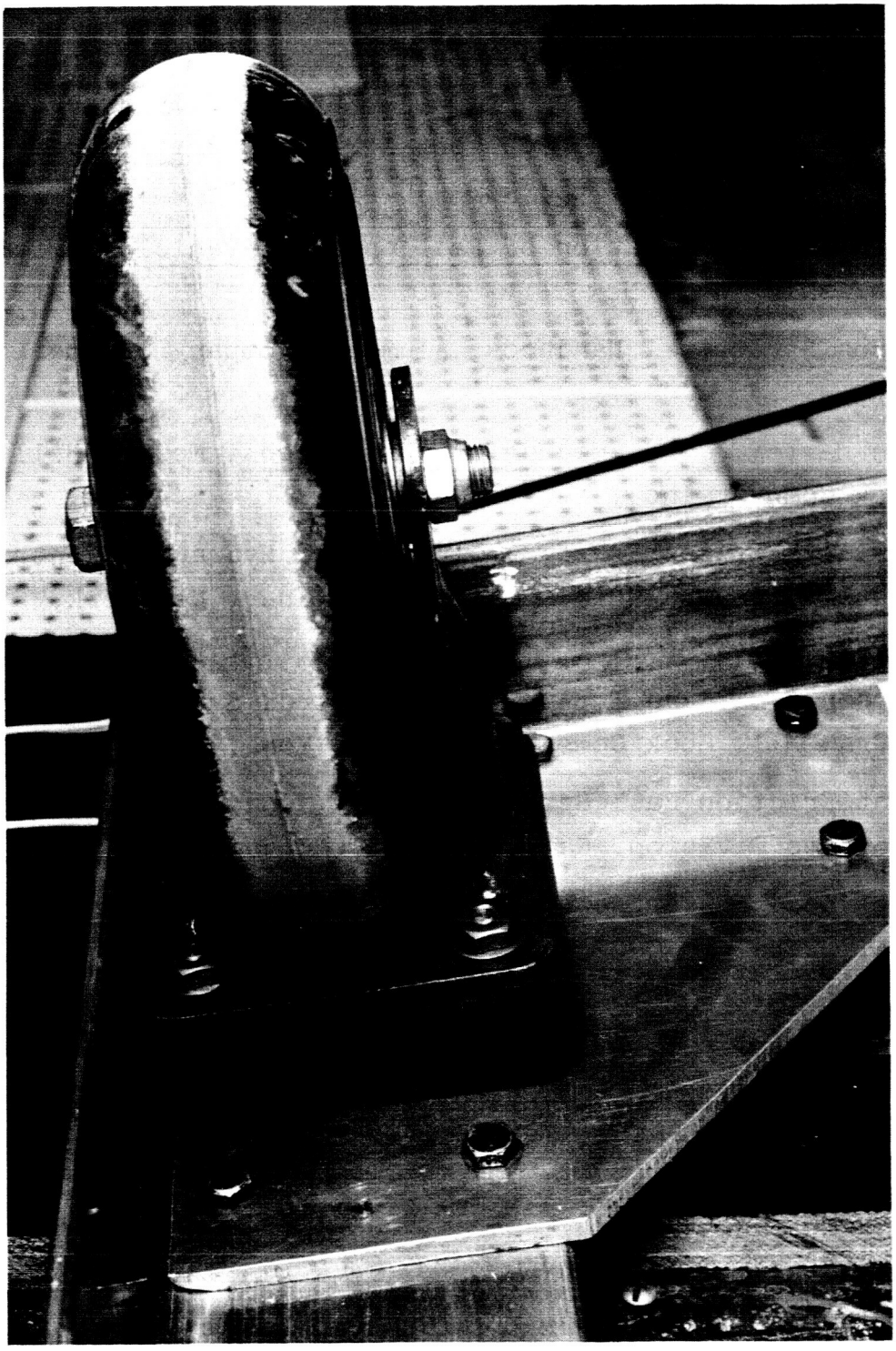

Fig. 7 Wheel Mount

REFERENCES

1. Walsh, E.G., "The Perception of Rhythmically Repeated Linear Motion in the Horizontal Plane," British Journal of Psychology Vol. 53, 439-445, 1962.

2. Cain, B.S., Vibration of Rail and Road Vehicles, Pitman Publishing Co., New York 1940.

3. Alcoa Structural Handbook, Aluminum Company of America, 1955.

4. Den Hartog, J.P., Mechanical Vibrations, McGraw-Hill Book Company Inc., New York, 1934.

5. Lewis, E.E. and Stern, H., Design of Hydraulic Control Systems. McGraw-Hill Book Company Inc., New York, 1962.

6. Gibson, J.E. and Tuteur, F.B., Control System Components, McGraw-Hill Book Company Inc., New York, 1958.

7. "Antifriction Ball Screws", Scully Jones. Special Products Division, Catalog 25-62, Chicago, Ill.

8. "Polynoid Linear Actuator," Skinner Precision Industries, Inc., Catalog 10-62, New Britain, Conn.